Proc. Lunar Sci. Conf. 8th (1977), p. 1697–1729.
Printed in the United States of America

Shock metamorphism of lunar and terrestrial basalts

RAND BRIAN SCHAAL
Lockheed Electronics Company, Inc., Houston, Texas 77058

FRIEDRICH HÖRZ
NASA Johnson Space Center, Houston, Texas 77058

Abstract—Lonar Crater (India) basalt and lunar basalt 75035 were shock loaded under controlled laboratory conditions up to 1000 kbar, the highest peak pressure obtained to date in successful shock recovery; most of the experiments were performed in a CO/CO_2 (1:1) environment evacuated to 10^{-7} torr. The classification scheme of progressive shock metamorphism devised by Kieffer *et al.* (1976a) for basalt from Lonar Crater also applies to lunar basalts. The major shock features are as follows: Class 1 (0 to ~250 kbar): brittle and plastic deformation; shock lamellae in plagioclase; Class 2 (~250 to ~450 kbar): complete phase transition of plagioclase to maskelynite; Class 3 (~450 to ~600 kbar): onset of feldspar fusion, predominantly along grain boundaries; Class 4 (~600 to ~800 kbar): vesicular and flowed feldspar melts with loss of original rock texture; Class 5 (>800 kbar): melting of pyroxene and ilmenite, in addition to plagioclase, generating "whole rock" melts. The lunar plagioclase ($\approx An_{87}$) in rock 75035 converts to maskelynite at approximately the same pressure as terrestrial plagioclase; however, lunar feldspar tends to be slightly more resistant to melting at higher pressures. Feldspar melting occurs in a wide pressure range, ~450–800 kbar, and basaltic "whole rock" melting requires shock pressures in excess of 800 kbar.

Out of a total of 152 basalt specimens in the curatorial thin section collection, only three rocks show shock effects as severe as Class 2 features. The natural features are identical to their experimental analogs. These three rocks, 15684, 12054, and 79155, are coincidentally draped with a thick glass of basaltic composition suggesting a genetic relationship between the impacts which produced the shock features and the glasses.

The scarcity of shocked basalt hand samples in contrast to the abundance of shock-produced agglutinates and homogeneous glass spheres in the lunar regolith attest to the dominant role of micrometeorite impact in the evolution of the lunar regolith. While agglutinates are produced by impacts into fine-grained soils, homogeneous glasses are generated by impacts onto solid rocks. Thus, statistical, geochemical surveys of such glass populations may help identify their parent lithologies. We also speculate that the overall glass content is lower in asteroidal regoliths and larger in Mercurian regoliths as compared to that in lunar regoliths.

INTRODUCTION

AGGLUTINATES, HOMOGENEOUS GLASS SPHERULES, and diaplectic feldspars are abundant in the lunar regolith and indicate a prolonged, repetitive nature of the lunar meteorite bombardment. To account for these abundant shock-produced particles, any given surface point must have suffered numerous impacts, even on relatively young maria. In order to improve our understanding of these cumulative shock effects it is essential to determine the effects of single impacts, i.e., the response of material during the passage of a single shock wave. This can be accomplished by examining materials shock loaded in the laboratory or lunar and terrestrial materials involved only in a single impact event. This study is a

petrographic investigation not only of experimentally shocked terrestrial and lunar basalts but also of naturally shocked lunar basalt samples which exhibit shock effects more severe than fracturing on hand specimen scales.

Previous investigations of experimentally and naturally shocked basalts serve as a framework for this study (James, 1969; Short, 1969; Chao *et al.*, 1970; Dence *et al.*, 1970; Schaal *et al.*, 1976; Kieffer *et al.*, 1976a). In particular, Kieffer *et al.* (1976a) distinguish five grades of progressive shock damage ranging from brittle failure to whole rock melting in naturally shocked basalt from Lonar Crater, India; absolute pressure calibration of the shock intensities was accomplished via controlled laboratory shock recovery experiments which duplicated natural effects from Class 1 through Class 4 in shots up to 642 kbar.

The first part of this report extends results of recovery experiments on Lonar basalt to approximately 1000 kbar, the highest shock pressures to date at which recovery was successful. The major part, however, describes shock features in a suite of analogous shock recovery experiments up to 1000 kbar on lunar basalt 75035 and in naturally shocked lunar basalts. The main objective is to document artificial and natural shock effects in lunar basalts. Moreover, the obvious parallelism between the Lonar and lunar studies makes it possible to contrast and compare terrestrial and lunar analogs in order to assess the fundamental effects of shock metamorphism on basaltic rocks. Discussion also focuses on the origin of variegated glasses which coat the shocked lunar basalts. Finally, we speculate on the role of shock in the evolution of asteroidal and Mercurian regoliths.

SHOCK RECOVERY EXPERIMENTS

A 20 mm flat plate accelerator is used in the shock-loading experiments. Details of this apparatus and the experimental procedures, including recovery of the shocked materials, are described by Hörz (1970), Gibbons *et al.* (1975), and Kieffer *et al.* (1976a). Lonar basalt target discs were 7 mm in diameter, 0.5 mm thick, and were shock loaded in an atmospheric vacuum of $2–4 \times 10^{-2}$ torr. Shots at 614 and 742 kbar, however, were only 6 mm in diameter, with the same thickness, and, more significantly, were shocked in a newly developed auxiliary vacuum chamber housed inside the normal, large impact chamber which is normally evacuated to 10^{-2} torr. The new auxiliary chamber may be pumped down to 10^{-7} torr and can be repeatedly flushed with any gas or gas mixture(s). The objective of this improvement is to better approximate ambient lunar impact conditions, especially oxygen fugacity, by repeatedly flushing with a CO/CO_2 (1:1) mixture and evacuating to as low as 10^{-7} torr during the actual experiment. The 614 and 742 kbar Lonar experiments served as test shots for this new vacuum system. They were performed at 2×10^{-6} torr of a CO/CO_2 (1:1) gas mixture.

Lunar basalt 75035 was selected for the shock experiments because of its unfractured and holocrystalline texture and its medium grain size (Longhi *et al.*, 1974), making each target disc of 5 mm diameter and 0.5 mm thickness fairly representative of the whole rock. Basalt 75035 in turn is fairly representative of the Apollo 17 low-K high-Ti basalts (Rhodes *et al.*, 1977; Longhi *et al.*, 1974; Papike *et al.*, 1976) and has geochemical and petrological affinities to some Apollo 11 and 12 basalts; thus, 75035 reflects a common lunar basalt type. Chip 75035,23 was sliced into thin wafers which in turn were cored with a diamond coring device to produce discs 5 mm in diameter which were ground and polished to 0.5 mm in thickness. Cutting, coring, and polishing were accomplished using high purity mineral oils and great care was taken to prevent contamination with H_2O. All ten recovery experiments utilized the new high vacuum system and CO/CO_2 (1:1) gas mixtures at pressures ranging from 10^{-5} to 10^{-8} torr. Additional details of the experiments are given in Tables 1 and 2. Chemical analyses were made with an ARL-EMX electron microprobe using the analytical techniques discussed by Schaal *et al.* (1976).

1977LPSC....8.1697S

Table 1. Experimental shock effects in basalt from Lonar Crater, India.

	—600 kbar—	Class 4	—800 kbar—	Class 5	
Shock pressure (±3%)	614 kbar	696 kbar	742 kbar	974 kbar	996 kbar
Texture	Microporphyritic texture destroyed; vesiculated	Ophitic texture destroyed; vesiculated	Mostly frothy; vesicular	Frothy; fragmented	Frothy; fragmented
Plagioclase	Flowed colorless glass; some vesicles; amorphous outlines	Flowed, colorless vesicular glass	Flowed, colorless, vesicular glass	Flowed colorless glass mixed with colored glasses; highly vesiculated	Flowed glass mixed in colored glasses; highly vesiculated
Pyroxene	Granulated; displaced along microfaults; reduced birefringence	Crushed; granulated; mosaicism	Granulated; fragmented; mosaicism	Flowed greenish glass mixed with colorless glass; relict grains granulated	Flowed, mixed, greenish glass; relict grains granulated
Ulvöspinel	Fractured	Fractured	Fractured	Granulated	Fragmented; mixed
Palagonite	Isotropic; flowed; reddish brown color preserved	Not recognizable	Isotropic; flowed; dark brown color	Isotropic; flowed; dark brown color	Not recognizable
Sample recovery	~75%	~30%	~75%	~40%—2 sections	~15%
Flyer plate	W*	W	W	W	W
Sample assembly	SS304†	SS304	FS77‡	FS77	FS77
Target cylinder	SS304	SS304	SS304	SS304	SS304
Projectile velocity (km/sec, ±1%)	1.87	2.08	1.66	2.07	2.11

*W = 99.9% W.
†SS304 = Stainless steel 304 (68% Fe, 21% Cr, 9% Ni).
‡FS77 = Fansteel 77(89% W, 7% Ni, 4% Cu).

Table 2. Shock effects in basalt 75035.

Shock pressure (±3%)	Class 1	—250 kbar—	Class 2	—450 kbar—	Class 3
	93 kbar	204 kbar	302 kbar	400 kbar	494 kbar
Texture	Ophitic texture preserved	Ophitic texture preserved	Ophitic texture preserved	Ophitic texture preserved	Ophitic texture preserved
Plagioclase	Grains fractured; some granulation; undulatory and patchy extinction	Intense fracturing; abundant micro faults; undulatory extinction	Partial to total conversion to maskelynite; grain outlines preserved; few fractures	All grains converted to maskelynite; grains fractured and deformed	All grains converted to maskelynite or plagioclase glass with incipient flow; intensely fractured and granulated; mosaicism
Pyroxene	Irregular and cleavage fractures; some granulation	Closed spaced irregular fractures; some granulation; mosaicism	Fractured and granulated; mosaicism	Intensely fractured and granulated; mosaicism	Intensely fractured and granulated; mosaicism
Ilmenite	Fractured; shock twins	Fractured; shock twins	Fractured; well developed shock twins	Fractured; disjointed; shock twins	Fractured; disjointed; shock twins
Cristobalite	Polygonal fractures; mosaicism	Irregular and polygonal fractures; mosaicism	Abundant irregular fractures; relict polygonal fractures; isotropic, diaplectic	Intensely fractured; relict polygonal fractures; isotropic; diaplectic	Intensely fractured; relict polygonal fractures; isotropic; diaplectic (~15% of mode)
Sample recovery	~80%	~85%	~90%	~30%	~65%
Flyer plate	Al2024*	SS304†	W‡	W	W
Sample assembly	Al2024	SS304	SS304	SS304	SS304
Target cylinder	Al2024	SS304	SS304	SS304	SS304
Projectile velocity (km/sec, ±1%)	1.10	0.97	1.03	1.31	1.56
Vacuum pressure (torr)	5.3×10^{-7}	1.2×10^{-6}	1.4×10^{-5}	3.1×10^{-8}	1.2×10^{-6}

*Al2024 = Aluminum 2024 (93.4% Al, 4.5% Cu, 1.5% Mg, 0.6% Mn).
†SS304 = Stainless steel 304 (68% Fe, 21% Cr, 9% Ni).
‡W = 99.9% W

Table 2. (*Continued*).

—600 kbar— Shock pressure (±3%)	Class 4 606 kbar	Class 4 668 kbar	Class 4 743 kbar	—800 kbar— Class 5 853 kbar	Class 5 999 kbar
Texture	Modified by flow, but recognizable	Modified by flow, but recognizable	Slightly frothy; texture destroyed	Frothy; ophitic texture destroyed	Frothy; glassy
Plagioclase	Slightly flowed colorless glass; sparse vesicles	Slightly flowed colorless glass; sparse vesicles	Flowed, vesicular, colorless glass	Frothy, flowed glass; dark color	Frothy, highly vesiculated flowed glass; mixed colored glass
Pyroxene	Granulated; mosaicism; reduced birefringence	Intensely fractured; mosaicism	Granulated; fragments disjointed	Melting on edges; granulated; mosaicism	Flowed, mixed greenish glass; relict grains fractured
Ilmenite	Fractured; disjointed; shock twins	Fractured; fragmented; shock twins	Fractured, granulated; shock twins	Fragmented; shock twins	Fragmented; shock twins
Cristobalite	Not recognizable	Fractured; partially fused; some relict polygonalism; isotropic	Fused to colorless silica glass; few fractures	Fused to colorless silica glass; amorphous outline	Colorless silica glass intermixed with other glasses
Sample recovery	~10%	~85%	~80%	~70%—3 sections	~15%—2 sections
Flyer plate	W*	W	W	W	W
Sample assembly	SS304†	SS304	FS77‡	FS77	FS77
Target cylinder	SS304	SS304	SS304	SS304	SS304
Projectile velocity (km/sec, ±1%)	1.86	2.01	1.67	1.80	2.12
Vacuum pressure (torr)	3.6×10^{-6}	3.0×10^{-6}	2.3×10^{-6}	2.3×10^{-5}	2.7×10^{-5}

*W = 99.9% W.
†SS304 = Stainless steel 304 (68% Fe, 21% Cr, 9% Ni).
‡FS77 = Fansteel 77 (89% W, 7% Ni, 4% Cu).

EXPERIMENTALLY SHOCKED LONAR BASALTS

Kieffer *et al.* (1976a) reported shock recovery experiments of Lonar basalt up to 642 kbar. We now describe additional experiments at 614, 696, 742, 974, and 996 kbar. Experimental conditions for shots 696, 974, and 996 kbar were identical to those in earlier shots (Kieffer *et al.*, 1976a). The main petrographic results are described in Table 1 and illustrated in Fig. 1. The observed progression of shock metamorphism is consistent with our previous studies. The boundary between Classes 4 and 5 may be placed at approximately 800 kbar. No whole rock melts are observed in the 742 kbar experiment, though vesicular plagioclase glass is abundant. In the 974 and 996 kbar experiments the total amount of material converted to whole rock melt is ≈80%; detrital pyroxene and

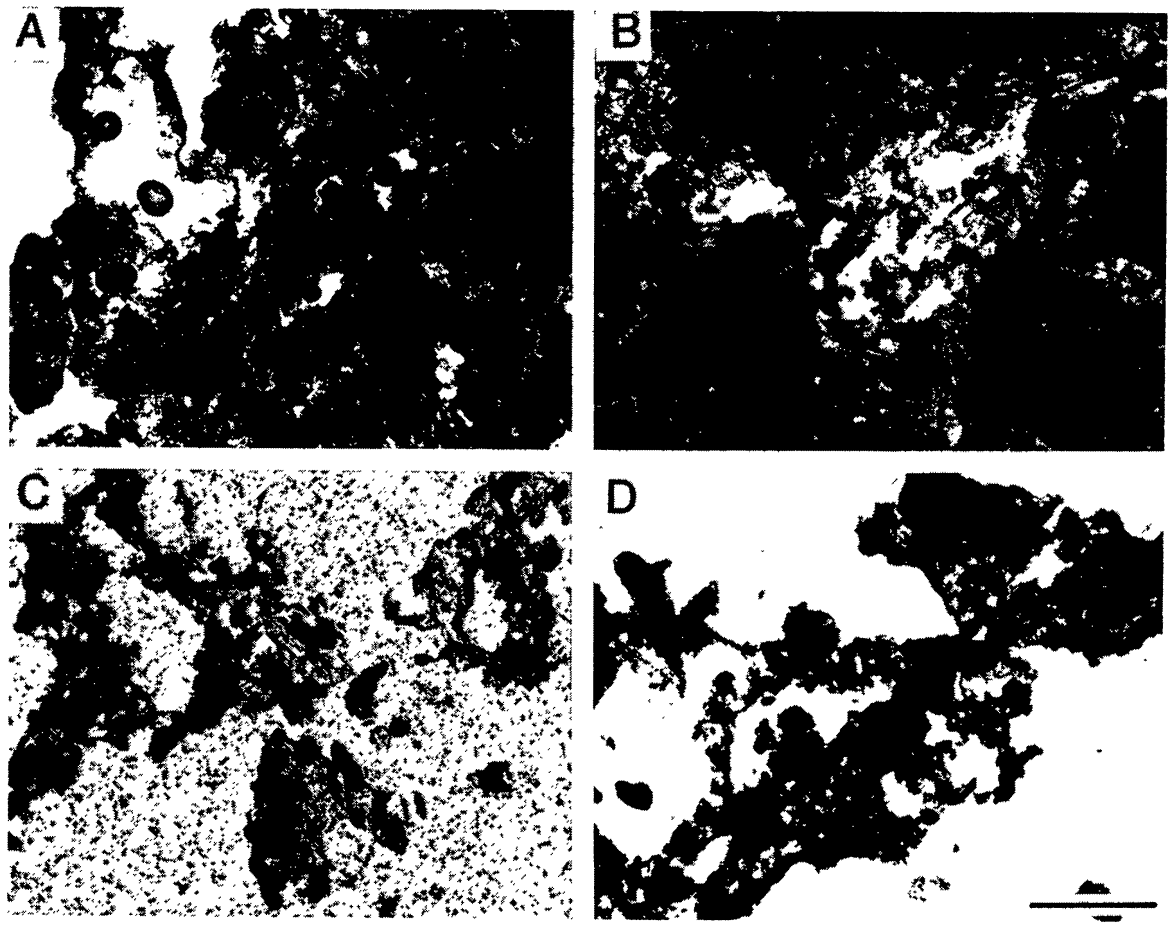

Fig. 1. Experimentally shocked basalt from Lonar Crater (India) representing shock Classes 4 and 5. Scale bar is 0.2 mm. (1A) Plane polarized transmitted light. Sample shocked to 696 kbar. Note vesiculation and flow of colorless plagioclase glass (left) and loss of porphyritic texture. Class 4. (1B) Sample shocked to 742 kbar. Note again vesiculation and drastic modification of original texture. All white grains are isotropic plagioclase glasses, either diaplectic or fused. Class 4. (1C) Sample shocked to 974 kbar showing frothy glass with schlieren and granulated inclusions of highly disjointed pyroxene. Most of the glass is "whole rock" melt, but some schlieren have strong affinities to monomineralic compositions. Class 5. (1D) Sample shocked to 999 kbar. Vesiculation and frothy texture are similar to those in 1C. Class 5.

ulvöspinel fragments are the only crystalline minerals remaining. Judging from these experiments, pressures in excess of 1 Mbar are necessary to cause complete melting of the Lonar basalt. These experiments also demonstrate that a variety of shock melting phenomena (e.g., selective melting of feldspars, vesiculation of feldspar melt, and onset of "whole rock" melting) develop in confined, seemingly random areas; the volumetric proportions of these glass types increase over a wide range of pressures, from ~400 to >1000 kbar. The shock experiments at 614 and 742 kbar performed in the new auxiliary vacuum system at 10^{-7} CO/CO_2 pressure fit perfectly well into the above scheme of progressive shock metamorphism. Varying oxygen fugacities compared to the Gibbons *et al.* (1975) and Kieffer *et al.* (1976a) as well as our 700, 974, and 996 kbar experiments at atmospheric vacuum of 10^{-2} torr did not lead to significant changes in the recovered products on our scales of observation. No shock reduction was observed, e.g., Fe°, and dissemination of sample assembly materials (Gibbons *et al.*, 1975) was largely eliminated by using a tungsten alloy (FS 77; Table 1) to contain the sample. Better controlled experiments with variable f_{O_2} are planned for the future, however, and constitute the main rationale for the development of the auxiliary vacuum system.

Experimentally Shocked Lunar Basalt

Unshocked basalt 75035 is a low-K, high-Ti, medium-grained, subophitic basalt described by Longhi *et al.* (1974). Their modal analysis gives 44% clinopyroxene, 33% plagioclase, 15% ilmenite, 5% cristobalite, 2% pyroxferroite, 1% native iron plus traces of troilite, and some mesostasis. Plagioclase and pyroxene are relatively unfractured (Fig. 2) and ilmenite is untwinned. Basalt 75035 samples were successfully recovered from ten experiments in which shock pressures ranged from 93 to 999 kbar.

Following the classification of Kieffer *et al.* (1976) the progressive damage and phase transitions of feldspar also serve as the best indicators of shock intensity in the lunar basalt. The most severe metamorphic effect in each thin section was used for classification of shock intensity and associated pressure calibration. The major shock effects observed in our experiments are summarized in Table 2 and illustrated in Figs. 3, 4, and 5.

Class 1 (<250 kbar): Shock features in feldspar and pyroxene grains are characterized by increasing fracturing up to approximately 200–250 kbar (Fig. 3A–D). Feldspar grains in rare cases display shock lamellae (e.g., Stöffler, 1972). Shock damage in ilmenite is characterized by abundant twinning even at 93 kbar, in agreement with Sclar (1971) and Minkin and Chao (1971). These features are typical of Class 1 features in the Lonar basalt (Kieffer *et al.*, 1976a).

Class 2 (~250–450 kbar): The characteristic Class 2 features are based on the conversion of plagioclase to diaplectic feldspar with reduced birefringence and, especially, to diaplectic feldspar glass, maskelynite, in the 302 kbar shot (Fig. 3E–H). Some diaplectic feldspar grains display shock lamellae. Pyroxene grains

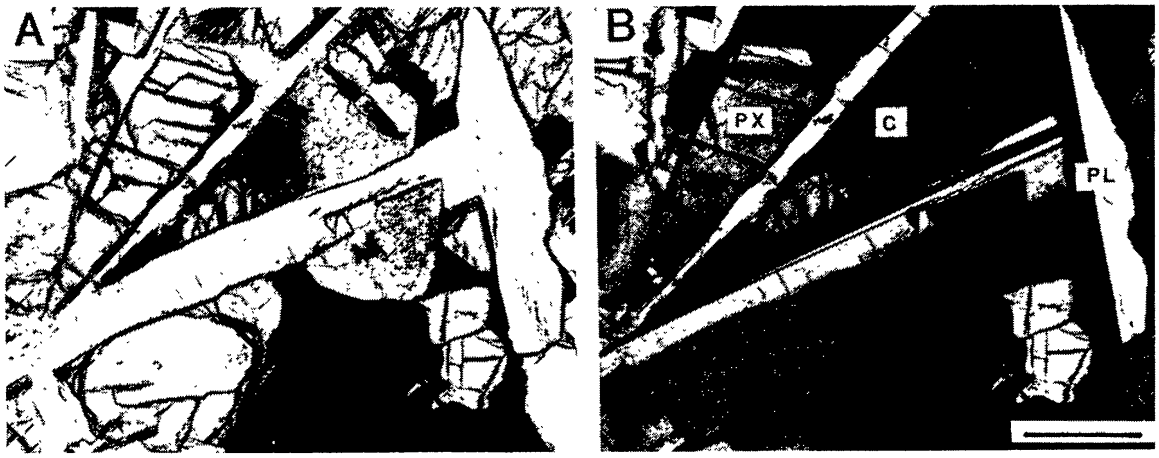

Fig. 2. Unshocked basalt 75035,76. Scale bar is 0.2 mm. (2A) Note medium-grained, subophitic texture; sparse fractures in pyroxene (PX); tabular shapes of plagioclase laths (PL); polygonal fractures in cristobalite (C); and interstitial ilmenite. Plane polarized light. (2B) Crossed polarizers. Note even birefringence in pyroxenes, undeformed twins in plagioclase, and nearly isotropic cristobalite.

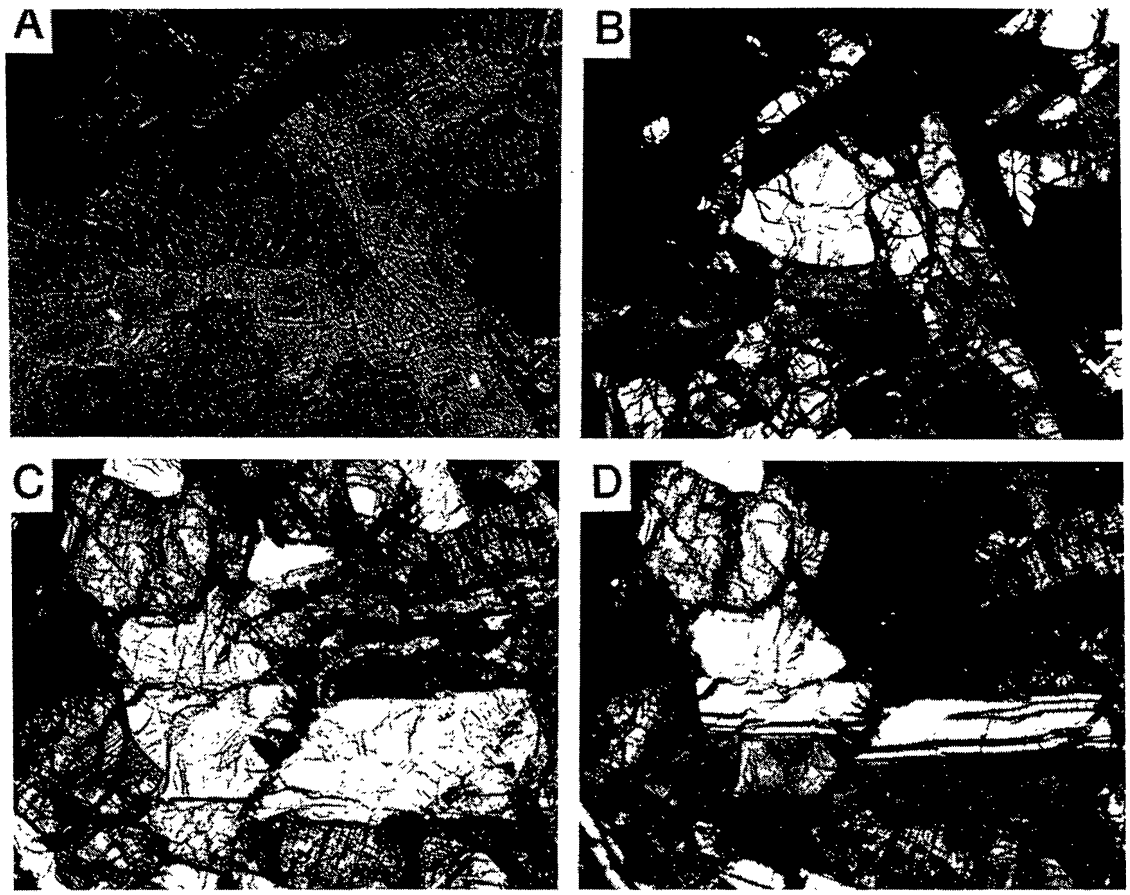

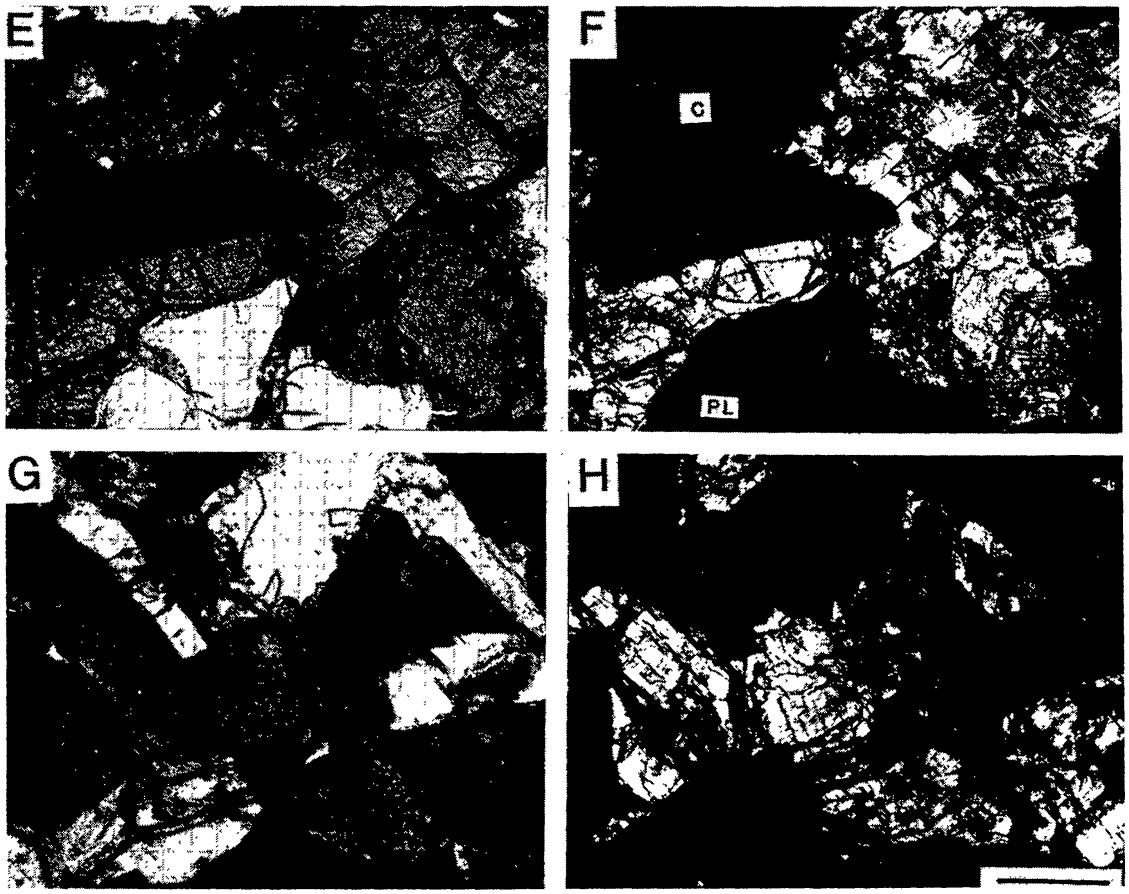

Fig. 3. Experimentally shocked lunar basalt 75035 representing shock metamorphic Classes 1 and 2. Scale bar for all photomicrographs is 0.2 mm. (3A) Class 1. Sample shocked to 93 kbar showing subophitic texture and abundant fractures in all component minerals. Plane polarized light. (3B) Same view as (3A), but with crossed polarizers. Note patchy extinction in plagioclase and pyroxene grains. (3C) Class 1. Sample shocked to 204 kbar. Note increased fine scale fracturing of all minerals. Plane light. (3D) Same view as (3C), but with crossed polarizers. Note distinct microfault offsets in twinned plagioclase, uneven extinction, and areas of decreased birefringence, i.e., almost isotropic patches. Deformation lamellae are visible in pyroxene grains, e.g., lower left. The cristobalite is also nearly isotropic. (3E) Class 2. Sample shocked to 302 kbar. Plane light. (3F) Same view as in (3E), but with polarizers crossed at 80°. Plagioclase (PL) is transformed into isotropic maskelynite containing sparse, conchoidal fractures. Note patchy extinction and shock lamellae in the highly fractured pyroxene grain to the upper right. Cristobalite (C) is also converted to diaplectic glass. (3G) Class 2. Sample shocked to 400 kbar. Plane light. (3H) Same view as (3G), but with polarizers crossed at 80°. All plagioclase and cristobalite are converted to diaplectic glasses. Ophitic texture is preserved. Mosaicism and patchy extinction are prominent in pyroxenes.

are progressively more fractured and granulated although grain boundaries are generally preserved. Ilmenite grains are twinned and in some cases bent.

Class 3 (~450 to ~600 kbar): The distinction between Class 2 and 3 features is subtle, but important. Class 3 feldspar is fused to a glass which shows signs of incipient flow (Fig. 4A–D). This selective melting of feldspar starts on grain

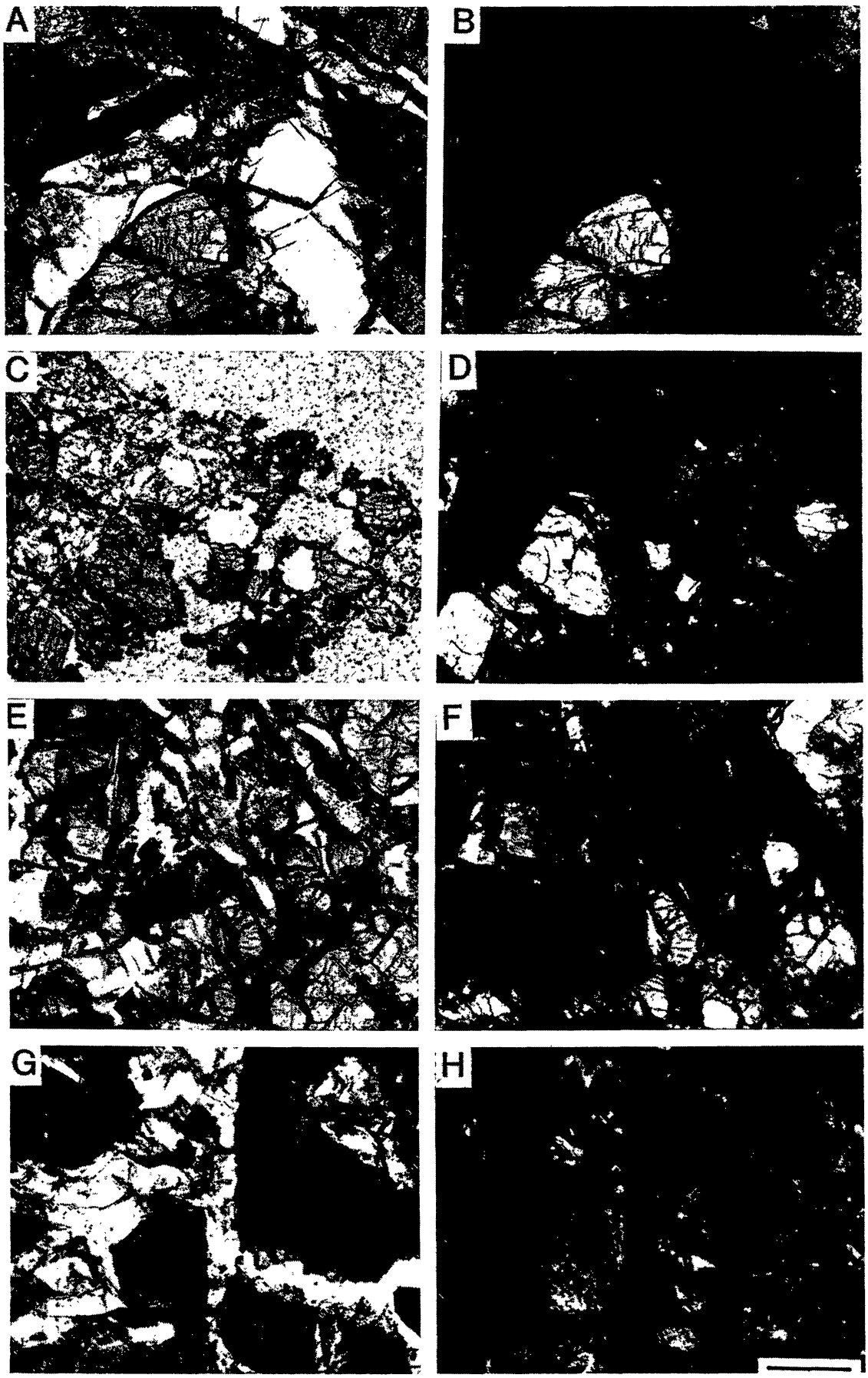

boundaries so that the glass conforms to the shape of fractured contiguous pyroxene grains, thereby modifying the initial rock texture. The total amount of feldspar glass increases with progressive pressure but does not amount to more than 10% of all feldspars present in the 494 kbar shot.

Class 4 (~600–800 kbar): The index for Class 4 features is the presence of vesicles in flowed, colorless, feldspar glass. Flow is prominent and may engulf several neighboring grains and penetrate fractures. Pyroxenes are more intensely granulated and fragments may be disjointed from their parent grains; some may be dragged along by the feldspar melt. Ilmenite is also highly granulated and disjointed. The overall rock texture has dramatically changed to an aggregate of intensely flowed feldspar melts and relatively large, detrital pyroxene, and ilmenite fragments.

Class 5 (>800 kbar): Between 800 and 1000 kbar all component mineral phases including pyroxenes and ilmenite show signs of melting (Fig. 5A–D). Thus, a large variety of glasses is observed, ranging from almost pure mineral compositions in individual schlieren to two or three phase mixtures and, finally, to whole rock melts. The 999 kbar recovery is dominated by whole rock melts; however, some 20% relict pyroxene and ilmenite fragments are dispersed in the flowed glass.

Throughout the range of progressive shock damage produced in these basalts composition variations of major mineral components was not detectable in microprobe analyses (see also Schaal *et al.*, 1976). Analyses showed that plagioclase glasses in samples shocked to pressures between 450 and 1000 kbar have compositions which are identical to those in maskelynites in shots between 250 and 450 kbar, in diaplectic plagioclase, <200 kbar, as well as in unshocked plagioclase (Table 3). Compositions of clinopyroxenes in the entire suite of shocked materials also demonstrate a coincidence with those in unshocked

Fig. 4. Experimentally shocked lunar basalt 75035 representing shock-metamorphic Classes 3 and 4. Scale bar is 0.2 mm for all photomicrographs. (4A) Class 3. Sample shocked to 494 kbar. Plane polarized light. (4B) Same view as (4A), but with polarizers crossed at 80°. Note complete conversion of plagioclase to isotropic glass with only slight modification of initial ophitic textures. Incipient melting is observed along some plagioclase boundaries. The only birefringent phase remaining is pyroxene. (4C) Class 4. Sample shocked to 606 kbar. Plane light. (4D) Same view as (4C), but with polarizers crossed at 80°. Plagioclase is totally converted to a colorless glass with slight vesiculation and incipient flow. Original ophitic texture is modified by flow. Large pyroxene grains are fragmented but retain normal birefringence. (4E) Class 4. Sample shocked to 668 kbar. Plane light. (4F) Same view as (4E), but with polarizers crossed at 80°. About 10% of plagioclase is fused into a vesicular, slightly flowed glass; the remaining plagioclase is maskelynite. Pyroxene and ilmenite grains are fragmented and disjointed. Initial rock textures are destroyed. (4G) Class 4. Sample shocked to 743 kbar. Plane light. (4H) Same view as (4G), but with polarizers crossed at 80°. Highly fluid plagioclase glass comprises a "matrix" enclosing pyroxene and ilmenite fragments. Pyroxenes are intensely fractured and show extreme patchy extinction (and on rare occasions an apparent decrease in birefringence). The glass is moderately vesiculated creating a slightly frothy texture.

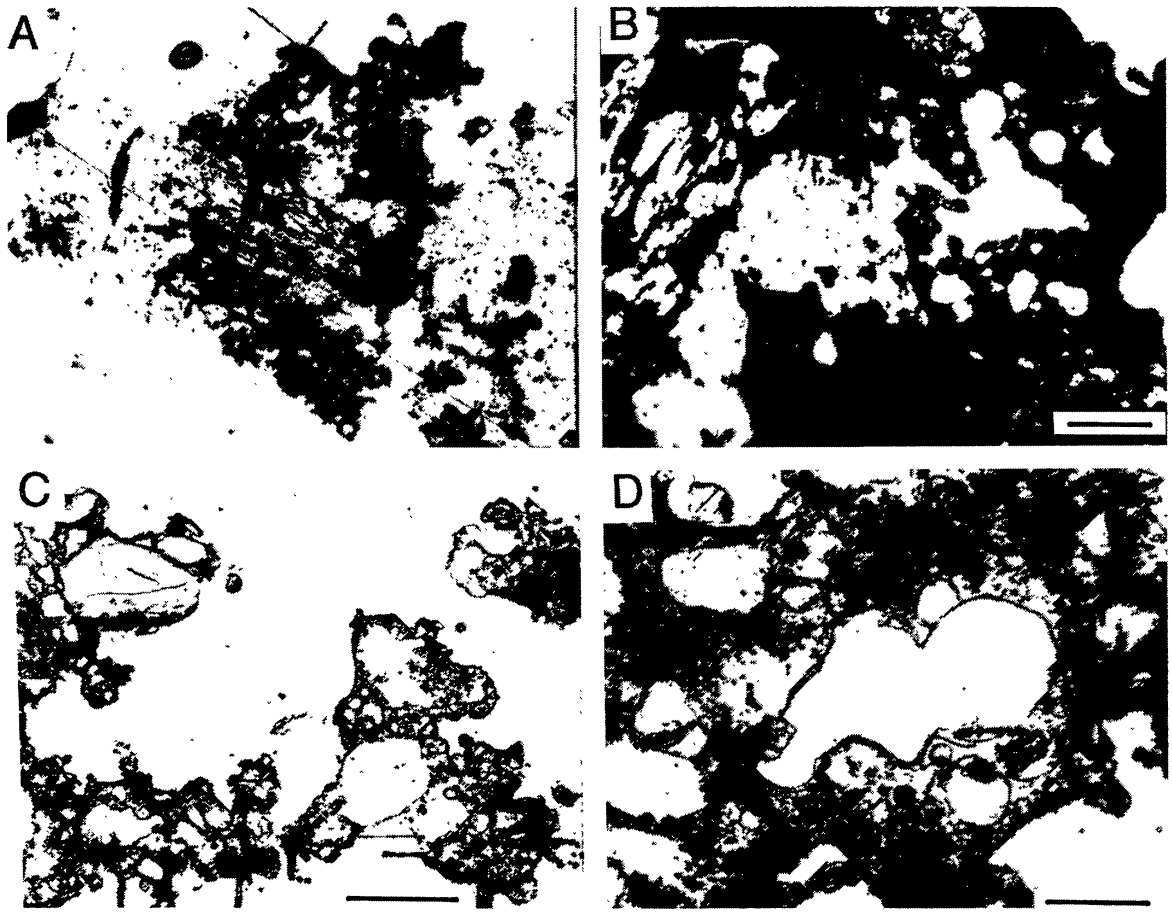

Fig. 5. Experimentally shocked lunar basalt 75035 representing shock-metamorphic Class 5. Transmitted plane polarized light in each photomicrograph. (5A) Sample shocked to 853 kbar. Note abundance of highly vesiculated, frothy glass, much of which is made up of "whole rock" melt according to microprobe analyses, though individual schlieren may be made up of monomineralic compositions. All feldspar is molten; however, pyroxene and ilmenite fragments are abundant. Scale bar for (5A) and (5C) is 0.2 mm. (5B) Enlargement of (5A) showing details of vesicles and flow features in glass. Scale bar is 50 μm. (5C) Sample shocked to 999 kbar. Note prominent, frothy texture of glass and detrital fragments of pyroxene and ilmenite grains. Relict grains may be aligned in flow features. Pyroxenes display reduced birefringence and edge melting. (5D) Enlargement of (5C) showing details of vesicles and flow features in glass. Scale bar is 50 μm.

samples (Fig. 6). In addition, the same is true for cristobalite. Nearly pure silica glasses (>96% SiO_2) are present as transparent schlieren within Class 5 glasses in samples shocked to 853 and 999 kbar, representing monomineralic remnants of cristobalite. Quantitative microprobe analyses in Class 5 samples were seriously impaired by several factors: (1) small quantities of sample recovered and extreme difficulties in preparing high quality polished thin sections, (2) intense, small-scale fracturing in relict crystalline grains, (3) small exposure area of frothy glass between vesicles, and (4) small-scale heterogeneity in mixed glasses prohibiting precise relocation of probe beam on successive runs. However, based on qualitative analyses we conclude that chemical fractionation caused by

Table 3. Compositions of experimentally shocked plagioclase, 75035.

Pressure	Average composition			No. of grains	Range An
	Or	Ab	An		
Unshocked	.5	16.6	82.9	15	82.9–88.0
Unshocked	1.7	17.6	80.7	1	—
93 kbar	.3	11.8	87.9	10	85.1–89.0
204 kbar	.5	13.7	85.8	10	80.5–88.3
302 kbar	.5	12.6	86.9	10*	79.7–89.0
400 kbar	.5	12.7	86.8	10*	81.4–89.1
494 kbar	.6	14.2	85.2	10*	80.5–89.3
668 kbar	.4	12.9	86.7	10*	82.3–88.8
853 kbar	.9	15.0	84.1	1†	—
999 kbar	.6	13.5	85.9	3†	84.3–89.2

*Maskelynite.
†Plagioclase glass.

selective alkali volatilization, by preferential assimilation, by crystal differentiation, or by other means induced by a single impact event is not appreciable in concentrations sensitive to probe analyses, in agreement with Schaal *et al.* (1976).

In summary, the shock features and associated peak pressures in lunar basalt 75035 are compatible with those observed in the Lonar basalt. The scheme of progressive shock metamorphism of Lonar basalt proposed by Kieffer *et al.* (1976) also applies to lunar basalt 75035. One subtle difference, however, is the

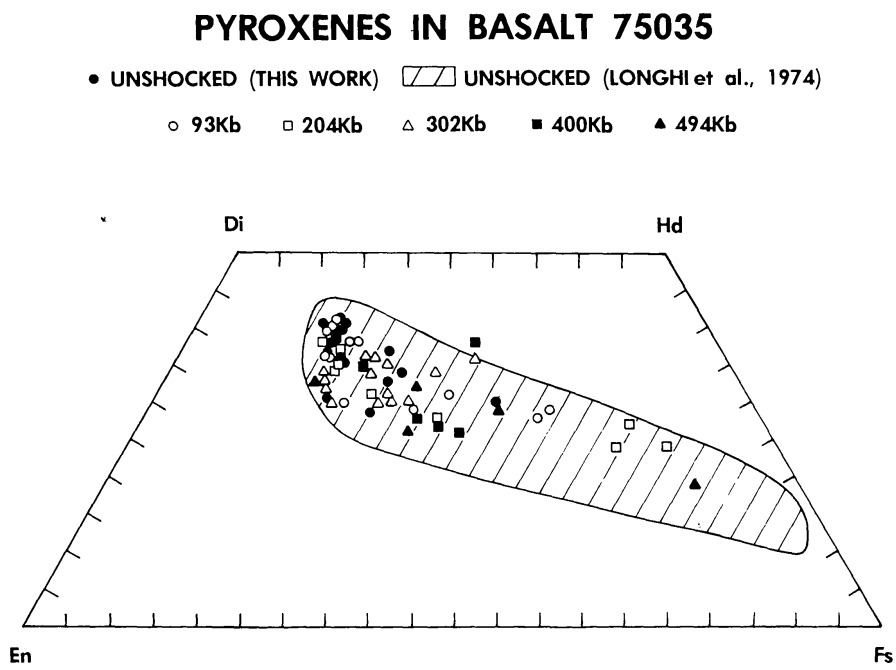

Fig. 6. Pyroxene quadrilateral showing range in compositions of shocked and unshocked pyroxenes in lunar basalt 75035.

somewhat increased stability of the lunar plagioclase which vitrifies at slightly higher pressures, i.e., at 250 kbar, and melts less profusely between 500 and 600 kbar than the terrestrial analog; some maskelynite grains are still present at 853 kbar. Thus, while the pressure brackets for the various shock grades are more or less identical, the amounts of feldspar and whole rock melts tend to be somewhat less in the lunar basalt at any given pressure. This may be understood in view of the higher melting point of the lunar anorthitic plagioclase (An_{87}; $\approx$1526°C) versus the Lonar plagioclase (An_{60}; $\approx$1474°C/1 bar, 0% H_2O; Bowen, 1913). Another possible factor could be the grain size; the Lonar basalt is significantly finer grained. Furthermore, Ahrens *et al.* (1977) report an equation of state for lunar basalt 70215 which has a lower shock impedance than corresponding terrestrial analogs and the "mixed phase" regime may possibly extend up to 800 kbar. In addition, Lonar basalts contain hydrous palagonite which may lower the overall melting temperature of the rock and/or the contiguous feldspar grains.

NATURALLY SHOCKED LUNAR BASALTS

Though it is commonly accepted that all lunar basalt specimens had experienced at least one meteorite impact that brought them to the surface for collection by the astronauts, it is also commonly agreed that the number of hand specimens displaying genuine shock features is extremely rare in the Apollo basalt collection (Chao *et al.*, 1970; Dence *et al.*, 1970; Engelhardt *et al.*, 1970; Quaide and Bunch, 1970). The mare basalt collection differs dramatically in this aspect from the suite of highland rocks which generally tend to be intensely shocked or even composed of impact melts. Classification schemes of progressive shock metamorphism for mare basalts in the past were based on particles recovered from the regolith and on inferences from terrestrial rocks, mostly granitic (Chao *et al.*, 1970; Dence *et al.*, 1970; Engelhardt *et al.*, 1970). We carried out a systematic search through the entire curatorial thin section collection which disclosed that out of 152 specimens available only three lunar basalts are shocked throughout with shock damage more severe than fracturing. These samples are 15685, 12054, and 79155 (we thank T. Usselmann for bringing sample 79155 to our attention), none of which were previously described in terms of shock metamorphic features.

Basalt 15684

Basalt 15684 is a pigeonite basalt chip approximately 8 × 6 mm in size. This sample was retrieved from an aggregate of rock chips cemented by a black glass matrix. Although a porphyritic subophitic texture is well preserved within the chip, 80–90% of the tabular to acicular plagioclase laths are isotropic maskelynite, accounting for 28% of the mode (Fig. 7A,B). Clinopyroxenes comprise 66% of the mode; pigeonite predominates (Fig. 8). Ilmenite accounts for ~8%, and trolite and kamacite are present in trace amounts; compositions are listed in

Table 4. Electron microprobe analyses of minerals and glasses in basalt 15684.

	(1)	(2)	(3)	(4)	(5)	(6)	(7)	(8)	(9)
SiO_2	48.03	51.47	53.84	48.61	—	48.17	50.68	39.64	47.20
TiO_2	.06	.65	.29	.96	52.33	.11	1.14	9.52	2.16
Al_2O_3	32.74	2.51	1.25	1.05	.04	32.01	4.67	6.26	9.56
FeO	.78	15.20	17.04	32.02	45.95	1.53	19.92	25.54	20.22
MnO	.00	.27	.28	.43	.29	.04	.26	.32	.27
MgO	.21	15.63	23.43	6.73	.13	.45	15.26	7.38	9.29
CaO	17.01	13.21	3.06	10.05	—	17.14	7.75	10.83	10.02
Na_2O	1.16	—	—	—	—	1.13	.28	.25	.41
K_2O	.06	—	—	—	—	.05	—	.08	.11
Cr_2O_3	—	.76	.66	.14	.07	.01	.68	.34	.49
Total	100.05	99.70	99.85	100.00	98.81	100.64	100.64	100.16	99.73

(1) Maskelynite, average of 10 grains.
(2) Augite, average of 4 grains.
(3) Pigeonite, average of 4 grains.
(4) Ferroaugite, average of 8 grains.
(5) Ilmenite, average of 7 grains.
(6) Colorless glass, average of 4 spots, 2 analyses for K_2O, and 2 for Cr_2O_3.
(7) Yellow green glass, single spot.
(8) Reddish brown glass, average of 7 spots, 2 analyses for K_2O, and 5 for Cr_2O_3.
(9) Greenish yellow to yellowish brown glass, average of 16 spots, 10 analyses for K_2O, and 6 for Cr_2O_3.

Table 5. Electron microprobe analyses of minerals and glasses in basalt 12054.

	(1)	(2)	(3)	(4)	(5)	(6)	(7)	(8)	(9)
SiO_2	46.44	46.97	49.58	50.15	51.36	—	49.12	40.71	43.27
TiO_2	.00	.00	1.40	1.28	.89	52.33	1.42	7.78	4.72
Al_2O_3	33.04	32.55	2.36	2.13	1.40	—	2.65	5.71	9.51
FeO	.54	.61	13.74	16.00	18.75	45.45	17.74	29.37	19.57
MnO	.00	.00	.24	.26	.26	—	.26	.32	.24
MgO	.28	.20	15.68	18.08	20.75	.17	13.92	1.92	9.22
CaO	18.42	18.75	14.15	9.61	4.85	—	12.77	10.06	11.45
Na_2O	.95	1.01	.02	.02	.01	—	.07	.19	.23
K_2O	.00	.01	—	—	—	—	—	—	—
Cr_2O_3	—	—	.79	.73	.57	—	.52	.13	.36
Total	99.67	100.10	97.96	98.26	98.84	97.95	98.47	96.19	98.57

(1) Plagioclase, average of 5 grains.
(2) Maskelynite, average of 5 grains.
(3) Augite, average of 4 grains.
(4) Subcalcic augite, average of 3 grains.
(5) Pigeonite, average of 3 grains.
(6) Ilmenite, average of 6 grains.
(7) Pale green glass, average of 4 spots.
(8) Reddish brown glass, single spot.
(9) Yellowish orange to light brown glass, average of 25 spots.

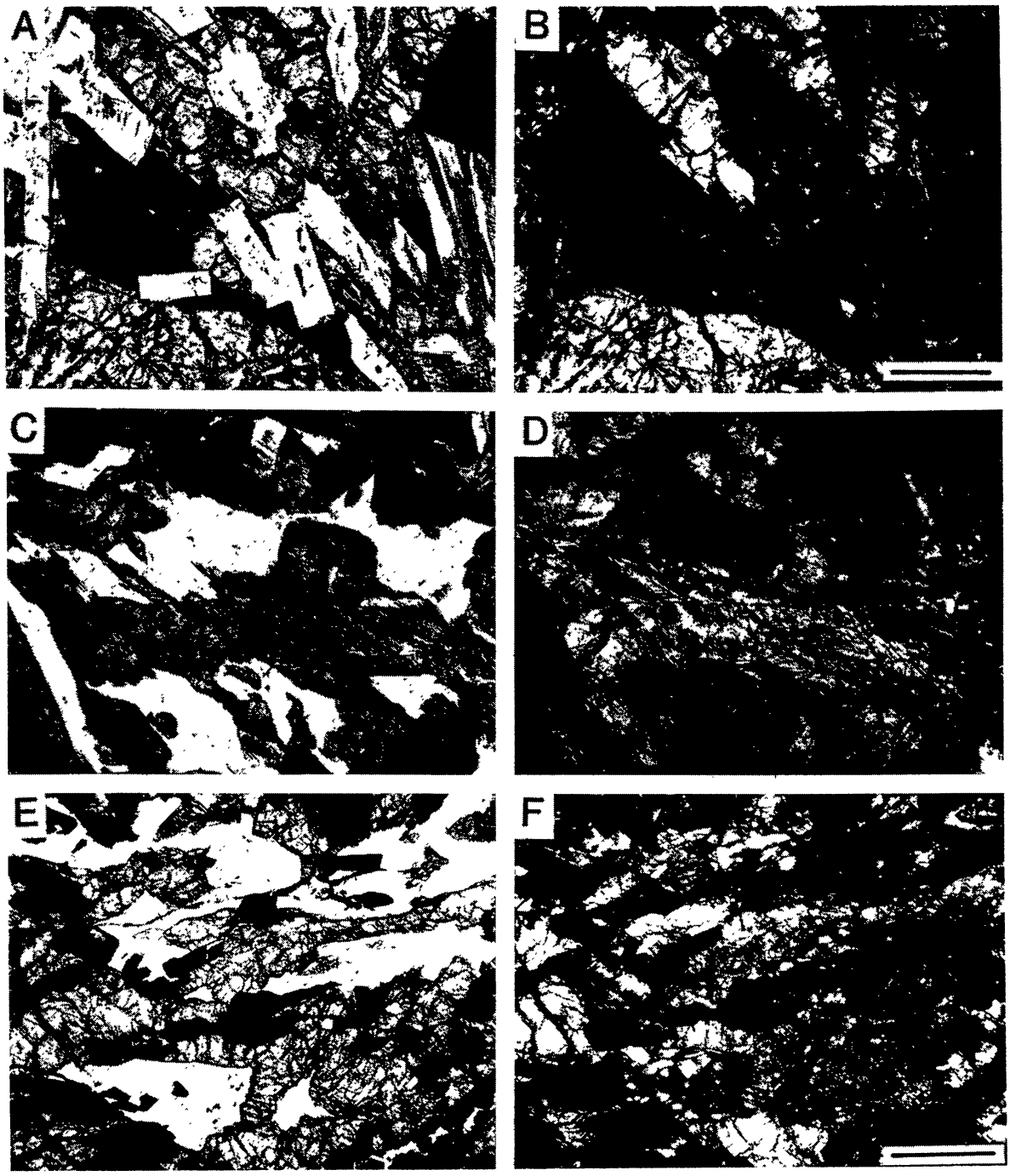

Table 4. Moderate shock effects are pervasive in thin section 15684,3. Prevalence of diaplectic feldspar glass throughout the section indicates a Class 2 shock history, with peak pressures less than 450 kbar. Pyroxene grains are granulated and mosaic; some contain closely spaced fractures and shock lamellae. The pressure distribution appears to have been uniform throughout this sample.

Basalt 12054

Ilmenite basalt 12054 (thin section 12054,79) contains 29% plagioclase, 62% clinopyroxene, 11% ilmenite, and traces of troilite and kamacite. Mode is based on a 3000-spot point count. The range of compositions of 40 plagioclase grains determined by microprobe analysis is from $An_{89}Ab_{11}$ to $An_{93}Ab_7$ with an average of $An_{91}Ab_9$ (Table 5). Analyses of 60 randomly selected pyroxene grains demonstrate a wide range of compositions between augite, subcalcic augite, pigeonite, ferroaugite, and subcalcic ferroaugite (Fig. 8). Augite and pigeonite are most abundant, consistent with trends reported for most Apollo 12 ilmenite basalts (Papike *et al.*, 1976). Individual pyroxene grains may be zoned with wide compositional variations between augite and subcalcic ferroaugite; exsolution lamellae are common. Ilmenite grains contain less than 1% MgO. Amorphous blebs of troilite and kamacite are generally closely associated or intergrown with metallic iron, perhaps representing a product of desulfurization of troilite (Gibson *et al.*, 1976; Brett, 1976) or a late-stage product of liquid immiscibility (Frondel, 1975, p. 20).

Weak to moderate shock effects representing Class 1 and Class 2 pressures are dominant petrographic features throughout the section (Fig. 7C,D). Diaplectic feldspars are highly fractured and exhibit pronounced undulatory extinction and decreased birefringence. Some contain up to three independently oriented systems of planar shock lamellae whose crystallographic planes are not measured at present. Maskelynite occurs throughout the section but is most abundant near one end where the sample is coated with glass. Analyses of 19

Fig. 7. Naturally shocked lunar basalts. (7A) Basalt 15684,3. The fine- to medium-grained subophitic texture shown in (7A) consists of tabular plagioclase-maskelynite laths, fractured pyroxene grains, and interstitial ilmenite grains. Plane polarized transmitted light. (7B) Same view as (7A) but with polarizers crossed at 80°. Note that plagioclase is partially to totally converted to maskelynite, typical of Class 2 shock intensity. Pyroxene grains display patchy extinction and are moderately fractured. Scale bar is 0.2 mm. (7C) Basalt 12054,79. Unfractured maskelynite grains are interspersed with intensely fractured pyroxene and ilmenite grains in medium-grained subophitic texture. Plane light. Scale bar is 0.5 mm for (6C–F). (7D) Same view as (7C), but with polarizers crossed at 80°. Some maskelynite grains contain relict domains of plagioclase crystal structure (white patches). Pyroxenes grains show patchy extinction. These features represent Class 2 shock intensity. (7E) Basalt 79155,60. This medium-grained ophitic basalt contains slightly fractured plagioclase-maskelynite grains and intensely fractured pyroxene and ilmenite grains. Plane light. (7F) Same view as (7E), but with polarizers crossed at 80°. Note relict crystalline domains in maskelynite grains and mosaicism in pyroxene grains, characteristic of Class 2 shock intensity.

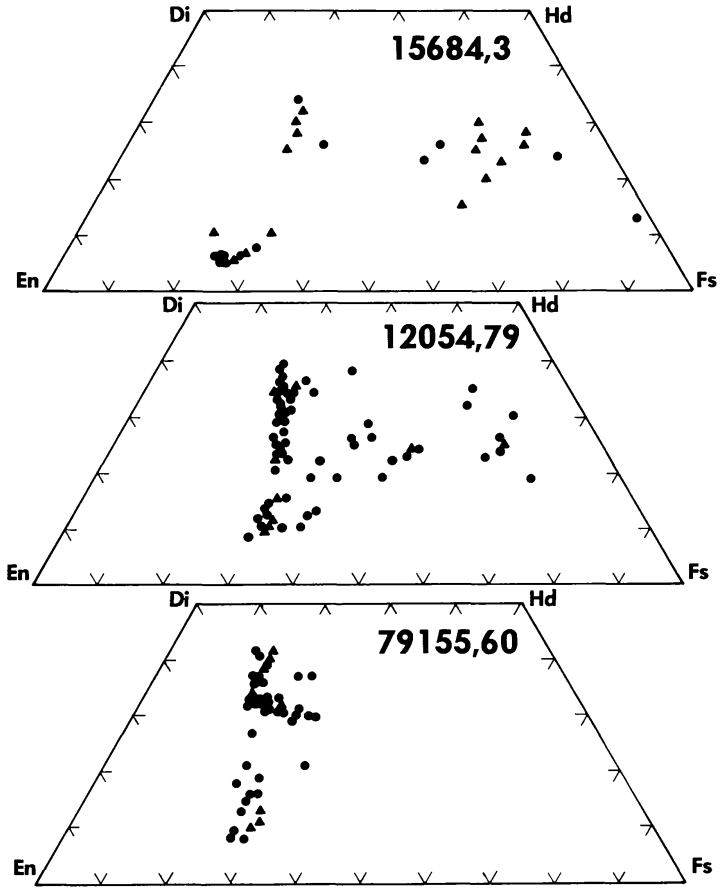

Fig. 8. Pyroxene quadrilaterals showing the variation of compositions of pyroxene grains in 15684,3, 12054,79, and 79155,60. Circles represent uncorrected compositions based on three element analyses only (Ca, Fe, Mg), while triangles represent corrected compositions based on nine element analyses presented in Table 4, 5, and 6, respectively.

maskelynite grains range from $An_{87}Ab_{12}Or_1$ to $An_{93}Ab_7$ with an average of $An_{91}Ab_9$, nearly identical with the unshocked plagioclase compositions (Table 5). Pyroxenes are intensely fractured or granulated and have suffered marked decrease in birefringence. Shocked ilmenite grains are also fractured and many display bent twin lamellae less than 15 μm wide. Thus, we estimate that peak shock pressures did not exceed 450 kbar within 12054.

Basalt 79155

Basalt 79155 is a high-Ti basalt. Thin section 79155,60 contains 19% plagioclase, 52% clinopyroxene, 24% ilmenite, and traces of olivine, troilite, and kamacite. Compositions of 28 plagioclase grains range from $An_{83}Ab_{17}$ to $An_{88}Ab_{12}$ with an average of $An_{87}Ab_{13}$ (Table 6). Augite and pigeonite are predominant pyroxenes and are strongly zoned; olivine (Fo_{69}) forms the core of some augite grains. Subcalcic augite is minor (Fig. 8) ilmenite grains contain less than 2% MgO (Table 6). Troilite and kamacite are usually intergrown.

Table 6. Electron microprobe analyses of minerals and glasses in basalt 79155.

	(1)	(2)	(3)	(4)	(5)	(6)	(7)	(8)	(9)
SiO_2	47.48	47.46	49.40	52.41	—	47.86	43.33	37.65	41.21
TiO_2	.06	.07	2.57	1.46	53.01	.08	7.26	16.35	9.38
Al_2O_3	33.30	33.26	3.62	1.96	.42	33.08	8.93	9.27	11.41
FeO	.35	.33	10.41	17.05	43.16	.55	16.40	20.44	17.05
MnO	.02	.02	.21	.28	.41	.02	.25	.34	.26
MgO	.28	.34	15.82	21.13	1.70	.27	10.57	7.95	7.92
CaO	16.83	16.91	16.91	5.60	—	16.62	11.20	9.18	10.78
Na_2O	1.39	1.37	.06	.00	—	1.45	.46	.38	.54
K_2O	.04	.03	—	—	—	.05	.06	.06	.10
Cr_2O_3	—	—	.69	.41	.90	—	.35	—	.32
Total	99.75	99.79	99.69	100.30	99.60	99.98	98.81	101.62	98.97

(1) Plagioclase, average of 5 grains.
(2) Maskelynite, average of 5 grains.
(3) Augite, average of 6 grains.
(4) Pigeonite, average of 3 grains.
(5) Ilmenite, average of 5 grains.
(6) Colorless glass, single spot.
(7) Yellowish orange glass, average of 5 spots, 2 analyses for K_2O, and 3 for Cr_2O_3.
(8) Reddish brown glass, single spot.
(9) Yellowish brown glass, average of 18 spots, 11 analyses for K_2O, and 7 for Cr_2O_3.

Rock 79155 displays an irregular spatial distribution of weak to moderate shock features and contains intergranular "pools" of vesicular glass randomly dispersed within the section. However, igneous textures are well preserved (Fig. 7E,F). More than half of the section contains fractured feldspar, pyroxene, and ilmenite grains with typical Class 1 cataclastic features. Some diaplectic feldspar grains display microfaults and planar shock lamellae. Interspersed among the fractured plagioclase crystals, accounting for the remainder of the section, are plagioclase grains which are partially to totally converted to maskelynite; one end of an individual grain may be crystalline (birefringent) and the other vitreous (isotopic) while retaining the initial crystal outline. Maskelynite grains signifying a Class 2 pressure regime are most abundant near the glassy zones. Most pyroxene grains are intensely fractured or granulated; undulatory extinction and mosaicism are widespread. Some pyroxenes display finely spaced shock lamellae, different from fractures, cleavages, or exsolution lamellae. Thus, unlike samples 15684 and 12054, which are fairly homogeneously shocked throughout the entire thin section, basalt 79155 displays general, Class 1 features and irregular pockets, a few millimeters across, of Class 2 features concentrated predominantly, though not exclusively, in areas where whole rock melts occur.

The similarity of these shock effects and those produced experimentally in rock 75035 indicate that the natural shock effects in lunar basalt can be simulated and successfully calibrated in the laboratory. The congruence of shock features in these two sets of samples is striking. We estimate that samples 15684, 12054,

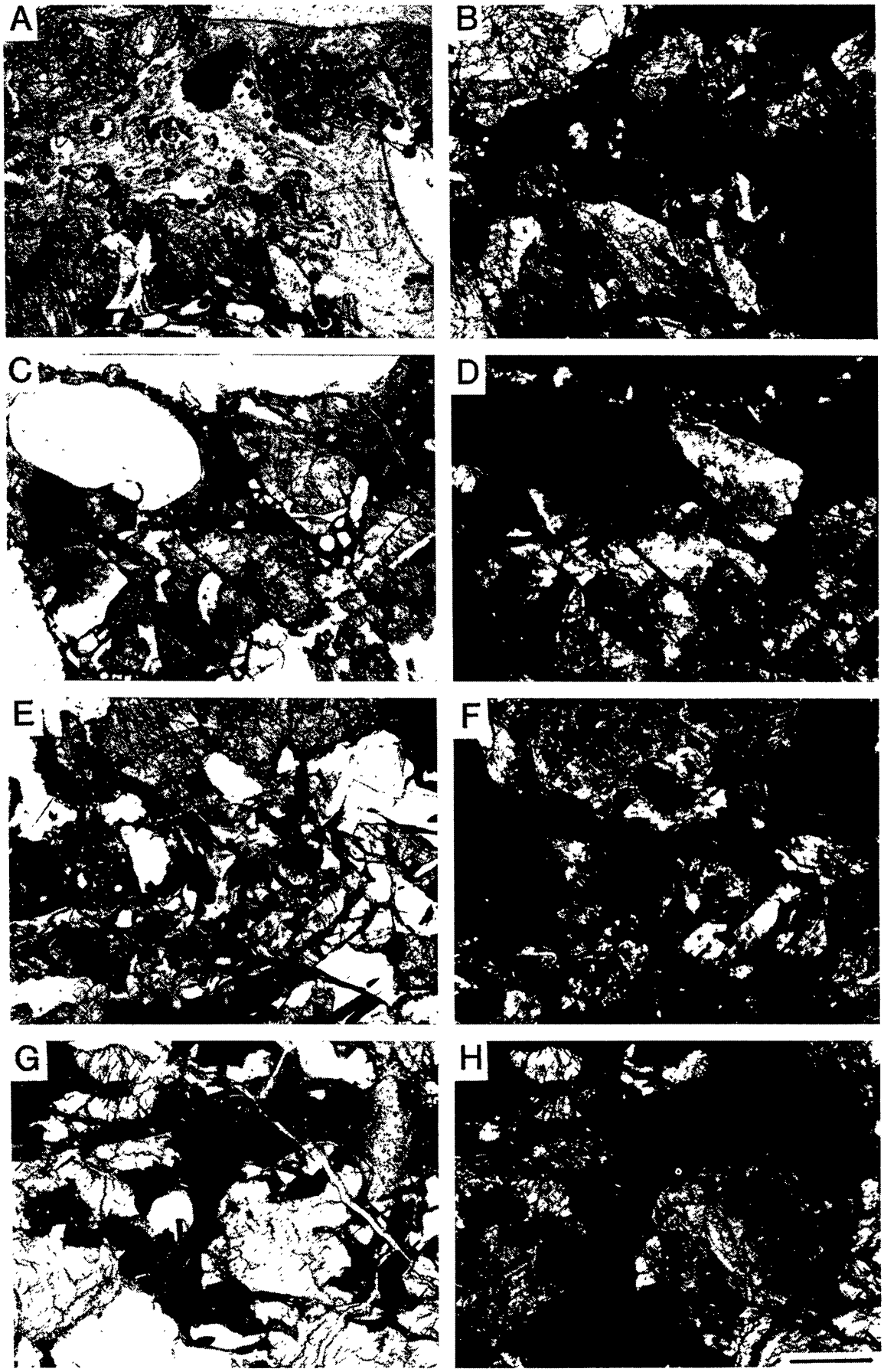

and 79155 have experienced maximum shock pressures on the order of 300–450 kbar.

Basaltic Glass Coatings

Each of the three naturally shocked basalts discovered in our survey is draped by a relatively thick, vesicular, variegated glass coating. The converse is not true, i.e., other basalts draped with glass are not necessarily shocked, e.g., rock 12017. We consider this correlation more than fortuitous and present textural and geochemical evidence that may illuminate the origin of these glass coatings. Shock melting by a single cratering event results in minor chemical modifications of the target material, as illustrated in experimentally produced whole rock melts, in the glass liner of a microcrater on rock 10085 (Schaal *et al.*, 1976), and in many other impact melts (e.g., Engelhardt, 1967; Simonds *et al.*, 1976). Therefore, it should be possible to establish the source area of these large glass coatings, especially to discriminate between a regolith or basaltic parent material.

15684 glass coating

A flowed vesicular glass coats nearly the entire perimeter of 15684 in thin section. The glass coating formed a thermal aureole in many of the grains it coats: edge melting is visible in pyroxene grains (Fig. 9A,B). The predominant colors in this glass are moderate yellow green (5GY 7/4; GSA rock-color chart). Flow features are accentuated with colorless and moderate reddish brown (10R 4/6) schlieren and with flow bands consisting of aligned kamacite, troilite, and schreibersite spherules up to 6 μm in diameter. An additional light brown (5YR 5/6) glass occupies a round patch within the basalt and a vesicular dark yellowish

Fig. 9. Glass coatings on naturally shocked lunar basalts. Scale bar is 0.5 mm in each photomicrograph. (9A) Basalt 15684,3. A flowed glass layer coats most of rock 15684 and contains vesicles, colored schlieren, flow bands of aligned metal spherules and shocked basaltic inclusions. Plane polarized light. (9B) Same view as (9A), but with polarizers crossed at 80°. Birefringence is visible in crystalline inclusions in isotropic glass. (9C) Basalt 12054,79. This highly vesiculated glass coats one side of rock 12054. The glass contains colored schlieren, flow bands of aligned metal spherules, and crystalline basalt inclusions. (9D) Same view as (9C), but with polarizers crossed at 80°. Birefringent pyroxene and basalt inclusions are recognizable in isotropic glass. (9E) Rock 79155,60. Colorless and colored glasses are interflowed in fractures within rock 79155. Colorless schlieren formed from plagioclase melts, and dark colored schlieren formed from ilmenite and pyroxenes. Plane light. Scale bar is 0.5 mm. (9F) Same view as (9E), but with polarizers crossed at 80°. Shocked basaltic fragments and vesicles are identifiable in glass. Note abundance of maskelynite. (9G) Rock 79155,60. This highly vesiculated, colored glass is injected into fractures in the rock interior through both maskelynite (lower center) and pyroxene grains (upper left). Multicolored schlieren enhance flow features. Plane light. Scale bar is 0.5 mm. (9H) Same view as (9G), but with polarizers crossed at 80°. The abundance of glass is made evident by the extent of the black area.

brown (10YR 5/2) glass fills fractures within the basalt. Glass colors are correlated to their compositions (Table 4). The majority of glass compositions cluster near typical Apollo 15 pigeonite basalt compositions on the ternary diagram (Fig. 10), though individual glass areas may constitute only a two or three phase mixture. However, most of the glass draping 15684 more closely resembles Apollo 15 basalt compositions than Apollo 15 soils, and, therefore, we conclude that it is derived from a (local?) basaltic substrate. Direct geochemical comparison with basalt 15684 is not possible because whole rock analyses for this specimen are not available.

12054 glass coating

A layer of yellowish orange to reddish brown glass up to 0.5 mm thick coats sample 12054 on the edge where shock effects are most severe. The glass did not form *in situ*, however. A thermal aureole less than 1 mm deep is visible in grains which the glass coats. Feldspar grains are partially to totally melted and show signs of incipient flow. Edges of most pyroxene grains coated with glass are rounded by edge-melting and form a veneer of grayish yellow green (5GY 7/2) to pale green (5G 7/2) glasses less than 0.1 mm thick with compositions nearly identical to those of underlying pyroxene grains. Flow schlieren in this "pyroxene glass" are traceable to distances of up to 0.4 mm. The major glass coating contains oblong vesicles up to 1.2 mm long (Fig. 9C,D). Pale yellowish orange (10YR 8/6) glasses are mixtures of plagioclase plus pyroxene com-

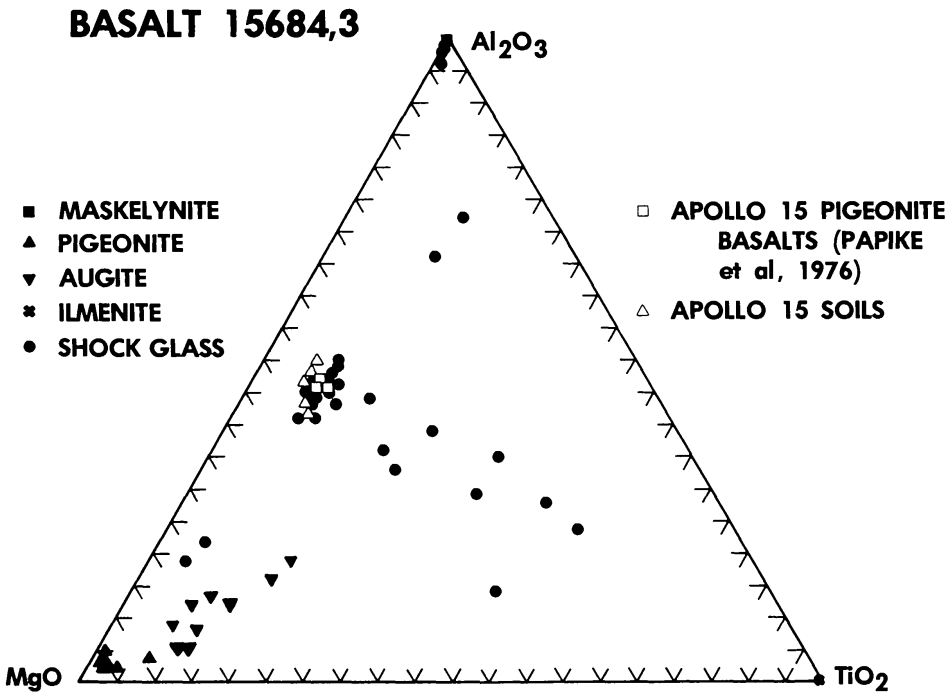

Fig. 10. Ternary diagram showing composition variation of shock glasses coating basalt 15684 with respect to the major rock-forming minerals. Glass compositions show closer affinity to other Apollo 15 pigeonite basalts than to Apollo 15 soils.

ponents; moderate reddish brown (10R 4/6) glasses are enriched in ilmenite components; and dark yellowish orange (10YR 6/6) to light brown (5YR 5/6) glasses are mixtures of all the basaltic components (Table 5). These prominant orange and brown glasses are most similar to the 12054 whole-rock sample (Rhodes *et al.*, 1977) or to a typical Apollo 12 ilmenite basalt in composition (Fig. 11); they show much less resemblance to Apollo 12 soil compositions (Frondel *et al.*, 1971). Thus, the 12054 glass is a flowed basaltic melt which thermally modified sample 12054 along its contact. The glass was deposited on 12054 as an impact melt splash derived from a basalt similar to 12054.

Both the thermally modified pyroxene grains and the green pyroxene glasses contain minute dendritic metal particles less than 1 μm across. These dendrites have medium reflectance. Furthermore, the brown glass coating contains two types of metal particles: one is the dendritic crystallites similar to those found in the green glass and in the pyroxenes. The other type consists of spherules with high reflectance and larger sizes than the dendritic particles. The dendrites are more abundant than the spherules. However, both particle types are too small to be accurately analyzed by conventional electron microprobe techniques.

79155 glass coating

A black glass coats the 79155 hand specimen but most of this crust is broken off the sample in thinsection 79155,60. Nevertheless, glass zones possibly related

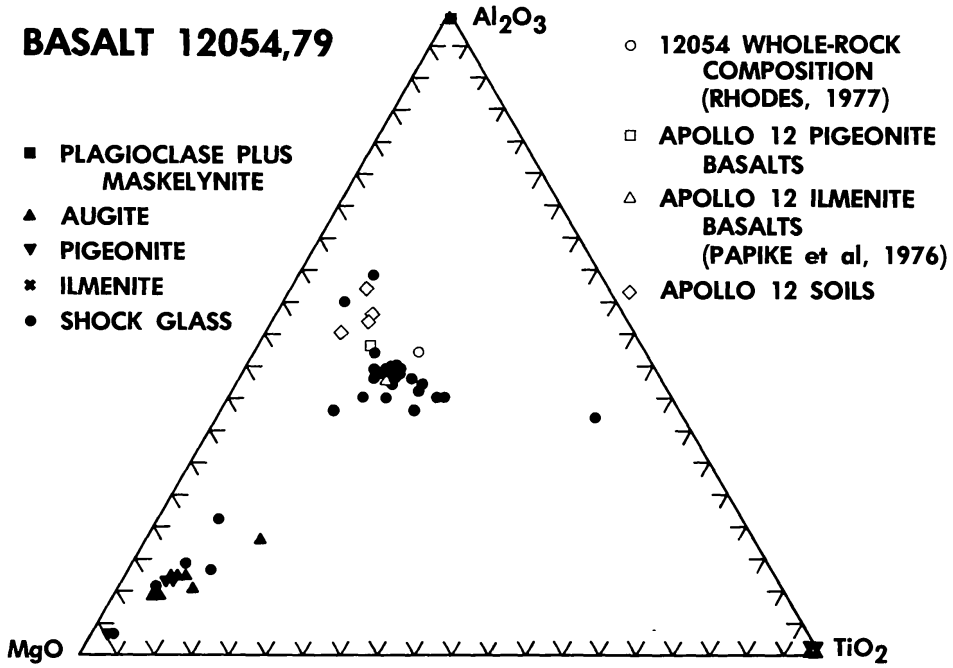

Fig. 11. Ternary diagram showing composition variation of shock glasses coating basalt 12054 with respect to the major rock-forming minerals. Glass compositions and the 12054 whole rock composition more closely resemble compositions of Apollo 12 pigeonite and ilmenite basalts than the local soils.

to the coating are preserved in intergranular spaced and in fractures covering approximately 6% of the interior of the section. The glass contains vesicles up to 0.5 mm in diameter and exhibits prominant flow features and schlieren accentuated by a wide range of colors and by flow bands of metal spherules less than 1 μm in diameter (Fig. 9E–H). Microprobe analyses again demonstrate the correlation of color with composition in the glasses: colorless glasses are composed predominantly of plagioclase components (relatively Al-rich): pale to dark yellowish or orange glasses (10YR 8/6 and 6/6) are enriched in pyroxene components (Mg-rich); moderate reddish brown glasses (10R 4/6) are enriched in ilmenite components (Ti-rich); and moderate yellowish brown glasses (10YR 5/4) are mixtures of feldspar, pyroxene, and ilmenite components (Table 6) in proportions the same as in the host basalt. Plots of these compositions on the ternary diagram show a closer affinity to Apollo 17 basalts than to Apollo 17 soils (Fig. 12). The slight K_2O enrichment in the brown glass (Table 6) is probably derived from K-rich mesostasis. XRF whole rock analysis gives a K_2O abundance of 0.06% similar to that in these brown glasses (Rhodes, pers. comm.). These findings are consistent with high alkali and silica contents reported in melt inclusions and in mesostasis (Weiblen and Roedder, 1976). Thus, we conclude that the glass within 79155 is a basaltic glass which was mobile but incompletely mixed; it certainly is not as homogeneous as glasses coating 15684 and 12054.

The origin of this basaltic glass is difficult to interpret because of a duality in the evidence. One line of evidence suggests an allochthonous origin; glass coats the surface of rock 79155 and fills fractures like thin feeder dikes to internal pools (Fig. 8). This suggests that a melt splashed onto the rock surface and

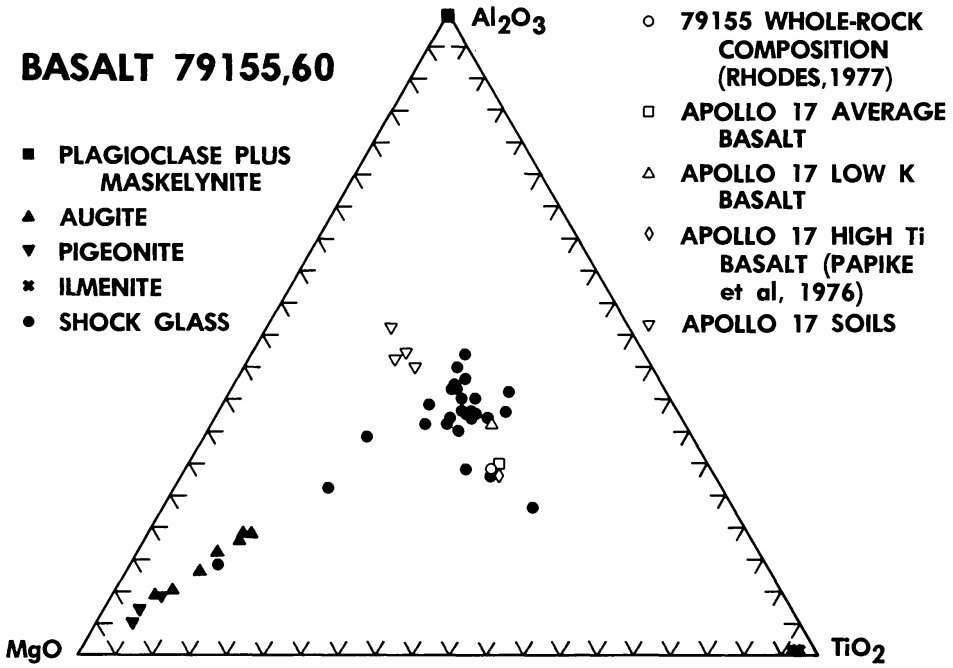

Fig. 12. Ternary diagram showing composition variation of shock glasses coating basalt 79155 with respect to the major rock-forming minerals. Glass compositions and the 79155 whole rock composition are more similar to Apollo 17 basalts than to local soils.

injected into fractures. Other evidence suggests that shock-induced melting may have formed the glass *in situ*. Nearly monomoneralic and bimineralic glasses are incompletely mixed and are located in patches where shock effects (i.e., fracturing and presence of maskelynite; see above) are most abundant. This suggests shock pressures and temperatures were focused along grain boundaries and formed melt in highly localized zones of pressure concentrations. The question whether the glass "ponds" formed *in situ* by shock melting or whether they are spatially and, thus, genetically related to the exterior glass splash remains unresolved.

We conclude that the glasses associated with each of these naturally shocked basalts was derived from basaltic targets most likely from the local substrate and not from their respective local regoliths.

Discussion

The following discussion purposely exceeds the scope of the specific experiments and observations reported above in order to summarize some of our previous shock experiments on basaltic targets and to discuss implications of these studies on the evolution of basaltic regoliths on other planetary surfaces.

Shock metamorphism of basalts

Our studies of the shock metamorphism of basaltic targets pursued over the last three years (Gibbons *et al.*, 1975; Schaal *et al.*, 1976; Kieffer *et al.*, 1976a) reveal a fairly close congruence of shock features between terrestrial and lunar basalts, despite some differences in phase chemistry and grain size. Within the limitations of our analytical techniques, the major diagnostic shock features occur at similar if not identical peak pressures and the various stages of shock metamorphism in solid basalts span similar pressure ranges. Furthermore, the congruence of shock effects in naturally and experimentally shocked specimens is striking; most naturally occurring petrographic features may be duplicated in the laboratory.

Feldspar remains the most diagnostic component phase for determining shock intensity. It displays a variety of deformation features and phase transitions which are highly sensitive to specific pressure histories. This is consistent with the stages of progressive shock metamorphism observed in terrestrial granitic rocks in which all framework silicates (quartz, K-feldspar, and plagioclase) may undergo basically similar phase changes (e.g., Stöffler, 1972). Lunar Ca-rich plagioclase is somewhat more resistant to melting than terrestrial plagioclase. Also, the mafic and oxide minerals in both rock types appear to display less dramatic and certainly less systematic deformation features and little or no phase transitions until shock temperatures are reached which are sufficient to produce "whole rock melts". The twinning of ilmenite under shock conditions constitutes a valid shock indicator at very low pressures in agreement with Sclar (1971) and Minkin and Chao (1971). The onset of "shock lamellae" in

pyroxenes is ill defined at the moment in our materials, but occurs at pressures of ~200 kbar. Their usefulness as pressure indicators, however, is limited because the onset of their formation approximately coincides with the more readily diagnosed formation of diaplectic feldspar glass. Furthermore, pyroxene lamellae are created through all degrees of shock up to the melting stage. Thus, the framework silicates appear to be best suited for pressure calibration of specific shock histories.

Examination of basalts shocked between 100 and 1000 kbar made it possible to characterize several stages in progressive shock melting. Shock-induced selective melting of plagioclase occurs over a very wide pressure range, starting with grain-boundary melting at ~450 kbar, resulting in pronounced flow and vesiculation at ~650 kbar, and finally contributes to mixed mineral melts and whole rock melts at >800 kbar. The amount of feldspar glass increases from a few localized occurrences at ~450–500 kbar to >90% at > 900 kbar; however, variations in the exact amount of melt present at intermediate pressures may vary, as exemplified by experiments on both the Lonar and lunar basalts. Thus, calibration of peak shock pressures in naturally shocked rocks between ~500 and 800 kbar is exceedingly difficult, because the occurrence of vesiculated feldspar glass at >650 kbar may be influenced by the amount of volatiles, e.g., H_2O, rather than by the specific P/T history. The production of feldspar melts mixed with diaplectic feldspar at shock pressures between 500 and 800 kbar demonstrates that the shock pressure distribution is heterogeneous on millimeter scales. Even the melts generated in the 974, 996, and 999 kbar shots contain relatively large amounts of pyroxene fragments and are characterized by numerous schlieren intermixed with "whole rock melts". Therefore, we conclude that the production of relatively homogeneous basaltic melts, such as the large glass coatings or the glass spheres in the Apollo collection, require $\gg$1000 kbar for their formation. Unfortunately, recovery attempts of Lonar basalt targets at ~1200 kbar were not successful, despite considerable efforts to improve the target container design.

Interpretation of the observed features with respect to equation of state (EOS) measurements on dense "basaltic" rocks (e.g., Vacaville basalt, Jones *et al.*, 1965 and Centreville diabase, McQueen *et al.*, 1967) is difficult because in-shock temperatures were not calculated and release adiabats were not measured. Release adiabats are available for lunar basalt 70215 only up to 200 and >1100 kbar pressure (Ahrens *et al.*, 1977). The EOS data available are, thus, not suitable to interpret specific features between 400 and ~1000 kbar in both the Lonar and the lunar basalts. These pressures are within the so-called "mixed phase" regime where normal and high density phases coexist; upon release high pressure phases convert to phases such as maskelynite or feldspar glasses, with densities lower than their initial densities. Plagioclase is the only mineral that demonstrably undergoes shock-induced density changes which are retained in recovery products. Pyroxene is relatively unaffected, though Ahrens and Gaffney (1971) interpret the onset of a "mixed phase" regime, i.e., the partial conversion to a high pressure phase, at 135 kbar in enstatite targets. Adiabatic

release of such a mixed phase regime should lead to significantly decreased densities of pyroxenes at pressures between 200 and 600 kbar, however, slightly decreased density as evidence by decreased birefringence is observed in our experiments only at pressures >600 kbar. Ilmenite also does not display any evidence of significantly reduced density at pressures as high as 900 kbar, although King and Ahrens (1976) observe a phase change at 320 kbar. Thus, plagioclase alone may bear the brunt of the shock compression and, as a consequence, may constitute the major variable in EOS measurements on basaltic targets.

Gibbons *et al.* (1975) report shock recovery experiments on particulate plagioclase and pyroxene mixtures as a simplified terrestrial analog to simulate the shock behavior of a lunar "basaltic" regolith. The resulting stages of progressive shock metamorphism differ significantly from those reported above on dense basalt targets. In accordance with theoretical considerations presented by Kieffer *et al.* (1976b) and Ahrens and Cole (1974), these porous aggregates yielded significantly more feldspar melt as well as whole rock melt at relatively lower pressures, e.g., at 514 kbar all feldspar is molten and ~50% of the entire sample was converted to an intergranular "whole rock" melt. We emphasize again the pronounced difference in the shock behavior between dense and porous targets, especially at 200–500 kbar pressures. Shock experiments on powdered basalt 75035 are planned to better characterize these differences.

Basaltic glass coatings

Our chemical analyses of the glass coatings on 15684, 12054, and 79155 compared with the bulk compositions of proximal basalt and regolith samples indicate that the glasses are derived from a basaltic substrate rather than from the local regolith. This interpretation strongly suggests that each glass coating is the product of a single impact. Estimates of the size of the parent crater are speculative, although the total penetration must have been deeper than the respective regolith thickness. Unfortunately, it is presently not possible to discern whether the glass coating and the solid-state shock effects were produced by the same impact or whether two separate impacts were responsible. However, the fact that the only shocked specimens recognized to date are also draped with a basaltic glass leads us to believe that the solid-state shock effects and the glass production are genetically related, and that they are the result of a single impact. Dating of the shock event(s) and the glass formation via $^{40}Ar/^{39}Ar$ laser probe methods (e.g., Plieninger and Schaeffer, 1976) may resolve the possibility of genetic relationship(s).

Furthermore, samples 15684, 12054, and 79155 may be valuable materials to study a variety of shock-related questions in lunar sample research; they are well suited to assess the possible disturbance of isotope systems used for absolute age dating, $^{40}Ar/^{39}Ar$ stepwise heating techniques, in particular, because the specimens are shocked to ~300–400 kbar during a single event. Also, a survey of the erasure of solar particle tracks and fission tracks by the passage of

a shock wave may be of interest. Microchemical analysis may evaluate the origin of the metal particles in the glass coating, by shock reduction in the absence of solar-wind derived hydrogen and/or by dissemination of meteoritic or indigenous metal. The value of these samples rests in the fact that they are shock products of a single impact.

Shocked lunar basalt and mare regoliths

The distribution of shock effects in the Apollo "basalt" collection is markedly bimodal in a comparison of hand specimens with regolith constituents. Out of approximately 152 hand specimens (>10 g) studies in our survey, only three samples displayed genuine shock features more severe than fracturing on hand-specimen scales. Small-scale shock effects attributed to microcraters on exposed rock surfaces (e.g., Schaal *et al.*, 1976) were not considered. In contrast, mare regolith constituents contain widespread shock features and abundant shock glasses which may commonly exceed 50% by volume (e.g., Heiken, 1974). Thus, the cumulative impact energy deposited into the regolith by micrometeroids is indeed dramatically higher than the energy expended into the substrate by larger meteorites (Gault *et al.*, 1974). The scarcity of "shocked" basalt hand specimens is in fair agreement with the amount of material shock metamorphosed during single cratering events (e.g., Hörz, 1969; Stöffler *et al.*, 1975; Pohl *et al.*, 1977).

Quaide and Oberbeck (1975) demonstrated that the overall growth of the regolith is accomplished by adding freshly excavated material on top of an existing debris layer; according to Stöffler *et al.* (1975) this material is in large part "unshocked". Therefore, it is highly probably that most regolith glasses, including agglutinates, were subsequently formed by micrometeoroid impact into fine-grained regolith (Mendell and McKay, 1975; Gibbons *et al.*, 1976; Hu and Taylor, 1977). Such conclusions are probably also applicable to the more homogeneous, often spherical, glass particles characterized chemically by Reid *et al.* (1972) and many others. They also formed from micrometeorite impact, like the "agglutinates", except that their target sites were solid rock surfaces, i.e., rock fragments scattered on the lunar surface. The shock experiments described may explain the marked absence of mafic glasses of monomineralic compositions in the statistical glass surveys (e.g., Reid *et al.*, 1972): pyroxene and ilmenite (possibly also olivine, which, unfortunately, was not present in 75035) start to melt under shock conditions only after most of the plagioclase is completely molten. The pyroxene and ilmenite melts, thus, are immediately in contact with feldspar melts and mechanical mixing is accomplished rapidly upon pressure release, forming "whole rock" melts. Such whole rock melts will dominate the glass population and slight chemical variations are expected, clustering around the whole rock composition. These considerations lend additional support to the conclusion that discrete clusters of glass compositions are related to the bounds of parent-rock compositions.

Asteroidal regoliths

We will now apply similar considerations to speculate on the lithologic properties of basaltic regoliths on planetary bodies other than the moon. In doing so, we must clearly separate the effects of a single impact onto a solid bedrock versus the effects of repetitive bombardment which inevitably creates progressively more comminuted and finer-grained particulate material.

First, we consider a single impact on a fresh basaltic surface in the asteroid belt where mean collision velocities are a few kilometers per second (Hartman, 1972). With Fig. 13 we estimate the intensity of shock effects created by impact either by a chondritic meteorite (basalt: density ≈ 3 g/cc) or by an iron meteorite (≈7 g/cc) on a basaltic target using a mean impact velocity of 5 km/sec. Peak pressures achieved with the basaltic projectile are on the order of 500 kbar, barely sufficient to selectively melt some feldspar components and to preserve pyroxene and oxide components. Solid-state shock effects are dominant features in the impact ejecta. However, impact with an iron meteorite at 5 km/sec creates peak pressures in excess of 800 kbar and produces significant amounts of feldspar melts with minor amounts of "whole rock" melts.

Next, what if subsequent impacts occur on progressively more comminuted deposits? Gibbons *et al.* (1975) reported that significant amounts of "whole rock" melt are generated at pressures as low as 400 kbar in fine-grained pyroxene-plagioclase mixtures. Thus, given sufficiently repetitive bombardment, significant amounts of fine-grained regolith would be generated, which in turn would lead to increased glass production, i.e., "agglutinates" in a textural and chemical sense (Mendell and McKay, 1975; Hu and Taylor, 1977). The absolute amount, of course, will depend on the cumulative impact history.

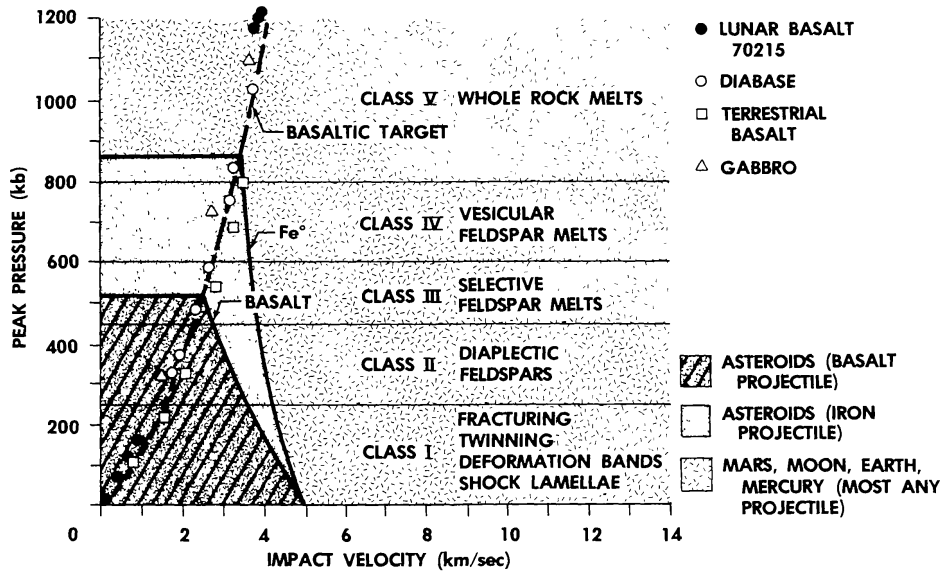

Fig. 13. Equation-of-state curves for "basaltic" materials in the pressure-particle velocity plane and projected shock damage in solid basalt targets using iron and basalt projectiles at 5 km/sec impact velocity typical for asteroidal collisions. (Lunar basalt: Ahrens *et al.*, 1977. All other equation-of-state data compiled by v. Thiel, 1967).

Recent spectral reflectance measurements of asteroidal surfaces, specifically the basaltic surface of Vesta (McCord *et al.*, 1970; Matson *et al.*, 1977), reveal a distinct lack of glassy surface materials. "Agglutinates" are also conspicuously absent in meteoritic "regolith" breccias (Kerridge and Kieffer, 1977). This lack of glass is consistent with our model of impact of a basaltic projectile on a solid basalt target at 5 km/sec (Fig. 13). Impact into fine-grained particulate targets is necessary to produce glass at that velocity (Gibbons *et al.*, 1975). Matson *et al.* (1977) discuss a variety of possible factors to account for the Vesta observations including total bombardment history, mean impact velocity and compositional differences. Our experimentally shocked lunar and Lonar basalts demonstrate that differences in modal compositions in basalts do not affect glass production significantly.

Matson *et al.* (1977) argue that the cumulative bombardment history on asteroids is rather similar to that of the inner planets. While this view may be correct for the early, large-scale bombardment history, it cannot be extended to micrometeoroids (the major lunar glass producer) because "large"-scale projectiles and micrometeoroids are derived from different sources. The micrometeoroid population is thought to originate predominantly, if not exclusively, from comets (e.g., Whipple, 1967; Zook, 1977). Micrometeoroid detectors on board Pioneer 10 and 11 measured a factor of 3 decrease in micrometeoroid activity going from 1.0 to 3.0 a.u. (Dohnanyi, 1975); conversely, recent HELIOS 1 measurements reveal a factor of approximately 20 more micrometeoroids at 0.3 a.u. than at 1 a.u. (Grün *et al.*, 1977). These measurements attest to an abundance of cometary particles in the inner solar system. In addition, the mean impact velocities vary systematically as a function of heliocentric distance (Dohnanyi, 1975; Grün *et al.*, 1977). Micrometeorite velocities in the asteroidal belt are uncertain at present, but Dohnanyi (1975) estimates that ~ 14 km/sec is a reasonable mean velocity. Thus, micrometeoroids are capable of generating impact melts in the asteroid belt, although the absolute micrometeorite flux and mean velocities there are lower than those on the lunar surface. These factors account for a relative lower glass production in the asteroid belt but do not totally prevent it.

Therefore, some other factor must be responsible for the apparent absence (= paucity?) of glass in the IR investigations of Vesta. We postulate that Vesta has a relatively coarse-grained surface deposit which prevents the formation of soil agglutinates. Micrometeoroid impacts on "pristine" rock surfaces generate relatively small amounts of glass and will not form agglutinates, the dominant lunar regolith glass. The grain size of such a deposit must be larger than the dimensions of typical microcraters (0.1–3 mm in diameter); therefore, we suggest that grain sizes on Vesta are greater than 1 cm.

Speculations concerning the possible origin of a regolith on Mercury must consider that both the spatial density and the impact velocity of micrometeroids are highest on Mercury than on all other planetary surfaces. Such impact conditions should create extremely glass-rich and finely comminuted surface deposits. Whether the total amount of glass on Mercury will exceed the amount

in the lunar regolith remains uncertain because the kinetics of glass formation strongly depend on the rate of replenishing the entire deposit with freshly excavated, pristine material and, thus, depends on the flux of relatively massive projectiles that penetrate bedrock (Mendell and McKay, 1975). If large-scale crater production rates are similar on Mercury and on the Moon (e.g., Gault *et al.*, 1975; Wetherill, 1975), then there will be approximately the same volume of pristine substrate material excavated per unit time; however such material exposed on the Mercurian surface will be more thoroughly reworked due to the higher micrometeoroid flux. In addition, large-scale secondary craters will be less widespread on Mercury than on the Moon (Gault *et al.*, 1975; Oberbeck and Aggarwal, 1977), allowing a relatively larger intercrater surface area to remain undisturbed per unit time; this in turn will lead to increasingly more comminution and reworking by micrometeoroids. Therefore, the Mercurian regolith may be finer grained and contain more agglutinitic glass than the lunar regolith.

Acknowledgments—We appreciate discussions with S. W. Kieffer and R. V. Gibbons and the skilled technical support from T. D. Thompson, Lockheed Electronics Co., Inc., Houston.

Portions of this study were supported by NASA grant NSG-7052 to UCLA and by the Lunar Science Institute, where RBS was a Visiting Graduate Fellow during the summer of 1976. The Lunar Science Institute is operated by the Universities Space Research Association under contract number NSR-09-051-001 with the National Aeronautics and Space Administration. This paper constitutes the Lunar Science Institute Contribution No. 285.

References

Ahrens T. J. and Cole D. M. (1974) Shock compression and adiabatic release of lunar fines from Apollo 17. *Proc. Lunar Sci. Conf. 5th*, p. 2333–2345.

Ahrens T. J. and Gaffney E. S. (1971) Dynamic compression of enstatite. *J. Geophys. Res.* **76**, 5504–5513.

Ahrens T. J., Jackson I., and Jeanloz R. (1977) Dynamic properties of ilmenite rich mare basalt and the relative ages of lunar cratered surfaces (abstract). In *Lunar Science VIII*, p. 1–3. The Lunar Science Institute, Houston.

Bowen N. L. (1913) The melting phenomena of plagioclase feldspar. *Amer. J. Sci.* **35**, 583.

Brett R. (1976) Reduction of mare basalts by sulfur loss. *Geochim. Cosmochim. Acta* **40**, 997–1004.

Chao E. C. T., James O. B., Minkin J. A., Boreman J. A., Jackson E. D., and Raleigh C. B. (1970) Petrology of unshocked crystalline rocks and evidence of impact metamorphism in Apollo 11 returned lunar sample. *Proc. Apollo 11 Lunar Sci. Conf.*, p. 287–314.

Dence M. R., Douglas J. A. V., Plant A. G., and Traill R. J. (1970) Petrology, mineralogy and deformation of Apollo 11 samples. *Proc. Apollo 11 Lunar Sci. Conf.*, p. 315–340.

Dohnanji J. S. (1975) Sources of interplanetary dust: Asteroids. In *Interplanetary Dust and Zodiacal Light* (H. Elsaesser and H. Fechtig, eds.), p. 187–205. Springer Verlag, New York.

Engelhardt W. v. (1967) Chemical composition of Ries glass bombs. *Geochim. Cosmochim. Acta* **31**, 1677–1689.

Engelhardt W. v., Arndt J., Müller W. F., and Stöffler D. (1970) Shock metamorphism of lunar rocks and origin of the regolith at the Apollo 11 landing site. *Proc. Apollo 11 Lunar Sci. Conf.*, p. 363–384.

Frondel C., Klein C., and Ito J. (1971) Mineralogical and chemical data on Apollo 12 lunar fines. *Proc. Lunar Sci. Conf. 2nd*, p. 719–726.

Frondel J. W. (1975) *Lunar Mineralogy*. John Wiley and Sons, New York. 323 pp.

Gault D. E., Guest J. G., Murray B. J., Dzurisin D., and Malin M. C. (1975) Some comparisons of impact craters on Mercury and the Moon. *J. Geophys. Res.* **80**, 2444–2460.

Gault D. E., Hörz F., Brownlee D. G., and Hartung J. B. (1974) Mixing of the lunar regolith. *Proc. Lunar Sci. Conf. 5th*, p. 2365–2385.

Gibbons R. V., Hörz F., and Schaal R. B. (1976) The chemistry of some individual lunar soil agglutinates. *Proc. Lunar Sci. Conf. 7th*, p. 405–422.

Gibbons R. V., Morris R. V., Hörz F., and Thompson T. D. (1975) Petrographic and ferromagnetic resonance studies of experimentally shocked regolith analogs. *Proc. Lunar Sci. Conf. 6th*, p. 3143–3171.

Gibson E. K., Usselman T. M., and Morris R. V. (1976) Sulfur in the Apollo 17 basalts and their source regions. *Proc. Lunar Sci. Conf. 7th*, p. 1491–1505.

Grün E., Fechtig H., Kissel J., and Gammelin P. (1977) Micrometeoroid data from the first two orbits of Helios I. *J. Geophys. Res.* In press.

Hartman W. K. (1972) *Moons and Planets.* Bogden and Quigley, New York. 404 pp.

Heiken G. (1974) A catalog of lunar soils. NASA Johnson Space Center, Curator's Office. 221 pp.

Hörz F. (1969) Structural and mineralogical evaluation of an experimentally produced impact crater in granite. *Contrib. Mineral. Petrol.* **21**, 365–377.

Hörz F. (1970) A small ballistic range for impact metamorphism studies. NASA-TN-D5787. 17 pp.

Hu H. N. and Taylor L. A. (1977) Agglutinate formation: Lack of chemical fractionation (abstract). In *Lunar Science VIII*, p. 463–465. The Lunar Science Institute, Houston.

James O. B. (1969) Shock and thermal metamorphism of basalt by nuclear explosion, Nevada Test Site. *Science* **166**, 1615–1620.

Jones A. H., Isbell W. M., and Maiden C. J. (1965) Measurement of the very high pressure properties of materials using a light gas gun. G. M. Defense Research Laboratories, Technical Report # TR65-84.

Kerridge J. F. and Kieffer S. W. (1977) A constraint on impact theories of chondrule formation. *Earth Planet. Sci. Lett.* **35**, 35–42.

Kieffer S. W., Phakey P. P., and Christie J. M. (1976b) Shock processes in porous quartzite: Transmission electron microscope observations and theory. *Contrib. Mineral. Petrol.* **59**, 41–93.

Kieffer S. W., Schaal R. B., Gibbons R. V., Hörz F., Milton D., and Duba A. (1976a) Shocked basalt from Lonar Impact Crater (India) and experimental analogues. *Proc. Lunar Sci. Conf. 7th*, p. 1391–1412.

King D. A. and Ahrens T. J. (1976) Shock compression of ilmenite. *J. Geophys. Res.* **81**, 931–935.

Longhi J., Walker D., Grove T. L., Stolper E. M., and Hays J. F. (1974) The petrology of the Apollo 17 mare basalts. *Proc. Lunar Sci. Conf. 5th*, p. 447–469.

Matson D. L., Johnson T. V., and Veeder G. J. (1977) Soil maturity and planetary regoliths: The Moon, Mercury and asteroids (abstract). In *Lunar Science VIII*, p. 625–627. The Lunar Science Institute, Houston.

McCord T. B., Adams J. B., and Johnson T. V. (1970) Asteroid Vesta: Spectral reflectivity and compositional implications. *Science* **168**, 1445–1447.

McQueen R. G., March S. P., and Fritz J. N. (1967) Hugoniot equation of state of twelve rocks. *J. Geophys. Res.* **72**, 4999–5036.

Mendell W. W. and McKay D. S. (1975) A lunar soil evolution model. *The Moon* **13**, 285–292.

Minkin J. A. and Chao E. C. T. (1971) Single crystal X-ray investigation of deformation in terrestrial and lunar ilmenite. *Proc. Lunar Sci. Conf. 2nd*, p. 237–246.

Oberbeck V. R. and Aggarwal H. R. (1977) Topographic analysis of lunar secondary craters of Copernicus and implications. *Proc. Lunar Sci. Conf. 8th.* Vol. 3.

Papike J. J., Hodges F. N., Bence A. E., Cameron M., and Rhodes J. M. (1976) Mare basalts: Crystal chemistry, mineralogy and petrology. *Rev. Geophys. Space Phys.* **14**, 475–540.

Plieninger T. and Schaeffer O. A. (1976) Laser probe ^{39}Ar–^{40}Ar ages of individual mineral grains in lunar basalt 15607 and lunar breccia 15465. *Proc. Lunar Sci. Conf. 7th*, p. 2055–2066.

Pohl J., Stöffler D., Gall H., and Ernstson K. (1977) The Ries impact crater. In *Impact and Explosion Cratering* (D. J. Roddy, R. O. Pepin and R. B. Merrill, eds.). Pergamon Press, New York. In press.

Quaide W. L. and Bunch T. E. (1970) Impact metamorphism of lunar surface materials. *Proc. Apollo 11 Lunar Sci. Conf.*, p. 711–729.

Quaide W. L. and Oberbeck V. R. (1975) Development of the mare regolith: Some model considerations. *The Moon* **13**, 27–55.

Reid A. M., Warner J., Ridley W. I., Johnston D. A., Harmon R. S., Jakeš P., and Brown R. W. (1972) The major element compositions of lunar rocks as inferred from glass compositions in the lunar soils. *Proc. Lunar Sci. Conf. 3rd*, p. 363–378.

Rhodes J. M., Blanchard D. P., Brannon J. C., Rodgers K. V., and Dungan M. A. (1977) Chemistry of Apollo 12 mare basalts: Magma types and fractionation processes. *Proc. Lunar Sci. Conf. 8th.* This volume.

Schaal R. B., Hörz F., and Gibbons R. V. (1976) Shock metamorphic effects in lunar microcraters. *Proc. Lunar Sci. Conf. 7th*, p. 1039–1054.

Sclar C. B. (1971) Shock-induced features of Apollo 12 microbreccias. *Proc. Lunar Sci. Conf. 2nd*, p. 817–832.

Short N. M. (1969) Shock metamorphism of basalt. *Modern Geology* **1**, 81–95.

Simonds C. H., Warner J. L., Phinney W. C., and McGee P. E. (1976) Thermal model for impact breccia lithification: Manicouagan and the moon. *Proc. Lunar Sci. Conf. 7th*, p. 2509–2528.

Stöffler D. (1972) Deformation and transformation of rock-forming minerals by natural and experimental shock processes I: Behavior of minerals under shock compression. *Fortschr. Miner.* **49**, 50–113.

Stöffler D., Gault D. E., Wedekind J., and Polkowski G. (1975) Experimental hypervelocity impact into quartz sand: Distribution and shock metamorphism of ejecta. *J. Geophys. Res.* **80**, 4062–4077.

Thiel v. (1966) Compendium of shock wave data. Lawrence Radiation Laboratory, Livermore, Report; U.C.RL-50108.

Weiblen P. W. and Roedder E. (1976) Compositional interrelationships of mare basalts from bulk chemical and melt inclusion studies. *Proc. Lunar Sci. Conf. 7th*, p. 1449–1466.

Wetherill G. (1975) Late heavy bombardment of the moon and terrestrial planets. *Proc. Lunar Sci. Conf. 6th*, p. 1539–1561.

Whipple F. L. (1967) On maintaining the meteoritic complex. *Smithson. Astrophys. Observ. Spec. Rep.* No. 239, p. 1–46.

Zook H. A. (1977) Temporal and spatial variations of the interplanetary dust flux. In *Papers Presented to the XXth Plenary Meeting of COSPAR and Associated Activities.* Tel-Aviv, Israel, 7–18 June 1977.